Chapter one

Introduction

Urinary system is also known as excretory system of human body. It is the system of production, storage and elimination of urine. Formation and elimination of urine is important for human body because urine contains nitrogenous wastes of the body that must be eliminated to maintain homeostasis. Nitrogenous wastes are formed by metabolic activities in the cells. These nitrogenous wastes along with excess of salts and water are combined in the kidneys to form urine. Urinary system is important for keeping the internal environment of the body clean. Urinary system maintains proper homeostasis of water, salts and nitrogenous wastes.

Kidneys are the major organs of urinary system. Formation of urine takes place in kidneys which are two bean shaped organs lying close to the lumbar spine, one on each side of the body. (S.Snell, 2007)**.**

Knowledge of kidney character is important for clinical assessment of renal disease. This study were to establish a normal range of values for kidney length and volume in normal Sudanese adults with no known history of renal disease and determine the usefulness of body mass index (BMI),body surface area (BSA), Glomerular filtration rate (GFR), Total body water (TBW),Creatinin Clearance (CrCl), Serum Creatinin Level (SrCr) for prediction of kidney characters. On the other hand touched this study to characterization of normal renal tissues in MRI images for Sudanese population using texture analysis. The renal tissues were classified into three classes as, cortex, medulla and pelvis using SGLD matrix.

1-1 Problem of study :

The kidney has variables dimensions among different people so there is a normal range all along between different nations and individuals. Therefore several nations they got their own index which is attributed to their body characteristics which include the height, weight, and gender and sometimes body mass index. In this essence Sudanese index is crucial as well as normal textural identity of the variable structure of the kidney will inspire and promote the potential capacity of the diagnostic capabilities.

- *Justification :*

General in literature the normal size of the kidney collateral to body character which made sometime exceed limit of normal range and this is estimated pathology similarity texture can be use differentiation between normal appear and pathological one.

There will be difference in kidney texture, length, volume in Sudanese population related habitués, and body index.

1-2 Research question :

- What is normal kidney measurement in Sudanese people?
- Does age affected the size of the kidney?
- Does gender affected the size of the kidney?
- Does weight and height affects the size of the kidney?
- What is optimum sub set of texture features that can classify the kidney?
- What are the kidney categories?
- What is accuracy of classification?

1-3 objective of study :

The general objective for this study was to characterizing normal kidneys using measurements and texture analysis for Sudanese people in MRI.

- *Specific objective :*

  - To assess renal size and texture feature.
  - To correlate the kidney volume with body mass index, age, habitués, gender.
  - To generate index for Sudanese and compare it with standard index.
  - To classify kidney into three classifications: cortex, medulla and Pelviocalyceal system.
  - To choose optimum sub set of texture feature that can classify kidney.
  - To measure the accuracy of the classifier.

1-4 Significant of study :

This study will highlight the measurements of the size of the kidneys using magnetic resonance images using disc summation method for renal volume and length are accurate and a reference values were established for adult Sudanese subjects and were well correlated with body parameters and renal function. And application of texture analysis in classification of normal kidney tissues by uses MRI. Therefore this study will be shed alight in the interpretation of the MR Images using computer facilities as computer-aided diagnosis.

1-5 Over view of study :

This study consisted of five chapters, with chapter one is an introduction which includes; problem of the study, question study objective and significance of the study. Chapter tow well present comprehensive literature review about different measurement studies and texture analysis and classification method ,while chapter three is a methodology which include material used to collect the data and method of data acquisition and analysis. Chapter four includes presentation of the result using tables and figures, finally chapter five included discussion, conclusion and recommendation.

Chapter two
Literature review

The urinary system consist of two kidneys situated on the posterior abdominal wall; two ureter, which run down on the posterior abdominal wall and enter the pelvis ; one urinary bladder located within the pelvis; and one urethra, which passes through the perineum. (S.Snell, 2007)**.**

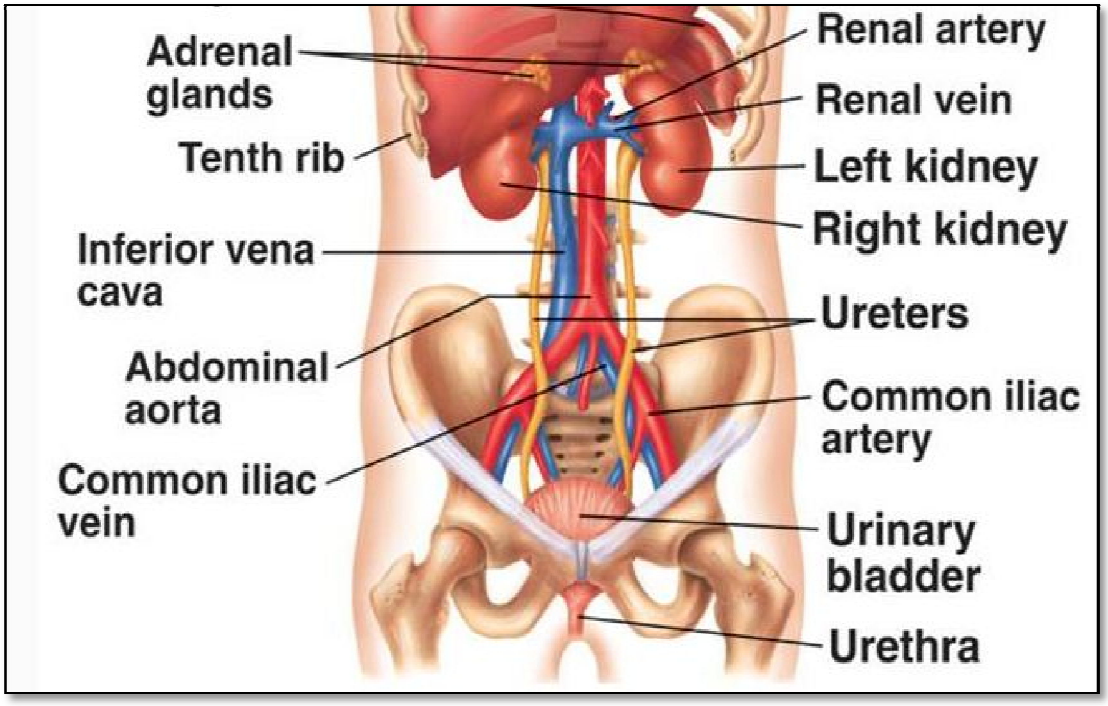

Fig (2-1) Urinary system (Adam biography2006)

2-1 Kidneys anatomy :

The two kidneys are lie behind the peritoneum high up on the posterior abdominal wall on either side of the vertebral column: they are largely under cover of the costal margin. Each kidney has a dark brown outer cortex and a light brown inner medulla. the medulla is composed of about a dozen renal pyramids , each having its base oriented toward the cortex and its apex , the renal papilla , projecting

medially .the cortex extends into the medulla between adjacent pyramids as the renal columns .extending from the bases of renal pyramids into the cortex are striations known as medullary rays. (S.Snell, 2007)**.**

The renal sinus, which is the space within the hilum, contains the upper expanded end of the ureter, the renal pelvis. This divides into two or three major calyces, each of which divides in to two or three minor calyces. Each minor calyx is indented by the apex of renal pyramid, the renal papilla.

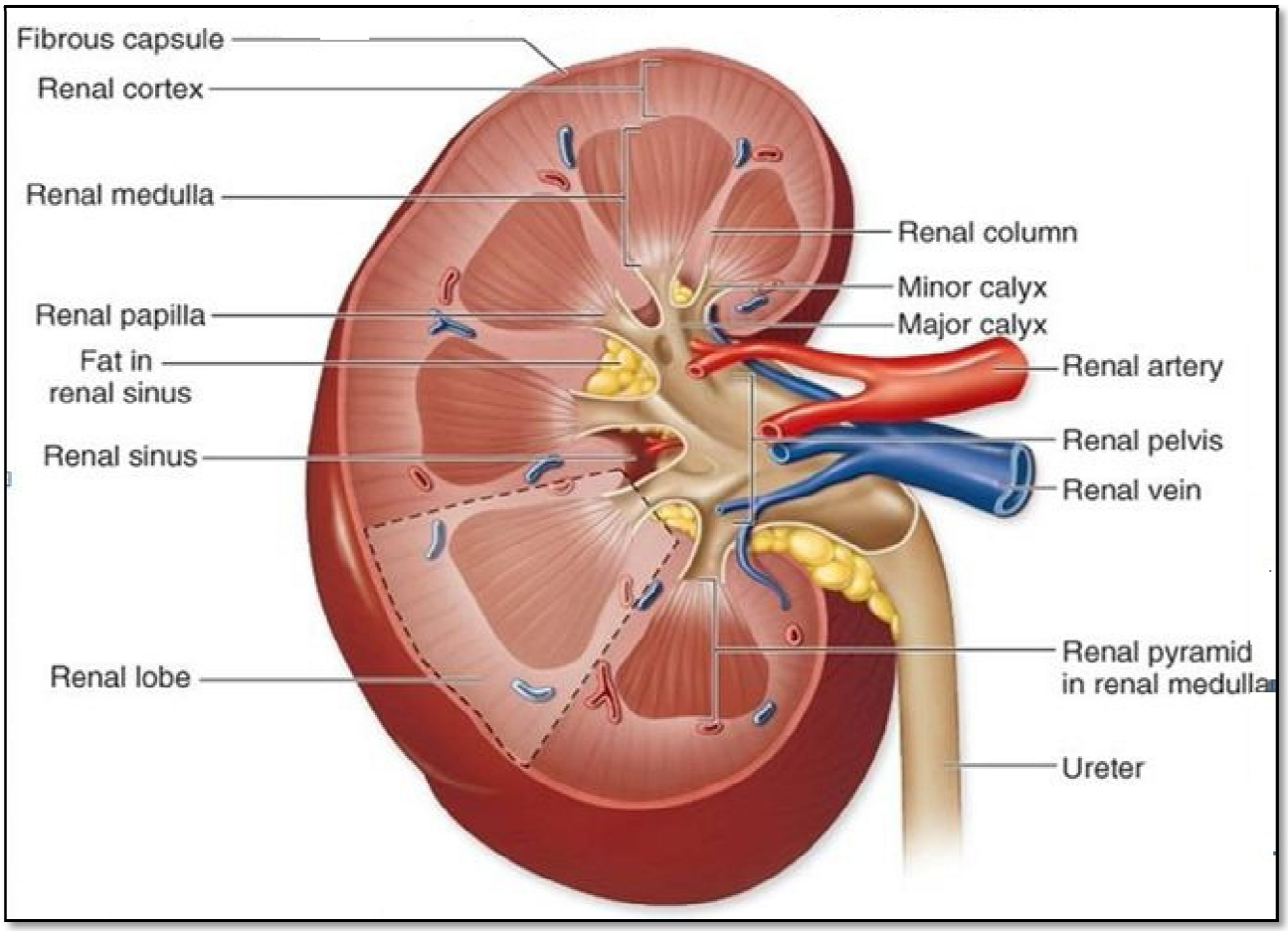

Fig (2-2) kidney anatomy (Adam biography2006)

2-1-1 Blood supply:

The renal artery arises from the aorta at the level of the second lumber vertebra. Each renal artery usually divides into five segmental arteries that enter the hilum of kidney, four in frontal and one behind the renal pelvis. They are distributed to different segments or areas of the kidney. Lobar arteries arise from each segmental artery. One for each renal pyramid. Before entering the renal substance, each lobar artery gives off two or three interlobar arteries .the interlobar arteries run toward the cortex on each side of the renal pyramid. At the junction of the cortex and the medulla, the interlobar arteries give off the actuate arteries, which arch over the bases of the pyramid .the actuate arteries give off several interlobular arteries that ascend in the cortex; the afferent glomerular arteries arise as branches of the interlobular arteries. The renal vein emerges from the hilum in front of the renal artery and drains into the inferior vena cava. (S.Snell, 2007)**.**

2-1-2 Nerve supply :

Renal sympathetic plexus. The afferent fibers that travel through the renal plexus enter the spinal cord in the tenth eleventh, and twelfth thoracic nerves. (S.Snell, 2007)**.**

2-2 kidney function :

The two kidneys function to excrete most of the waste products of metabolism. They play major role in controlling the water and electrolyte balance within the body and in maintaining the acid-base balance of the blood. The waste products leave the kidneys as urine, which passes down the ureter to the urinary bladder, located within the pelvis. The urine leaves the body in the urethra. (Mark H, Beers M 2010).

2-3 Kidney Diseases:

The kidney disease is generally divided into two types of congenital and acquired, congenital diseases such as Renal agenesis {solitary kidney}, Ectopic kidney, Horse shoe kidney, Cross ectopic, Duplication of ureter and renal pelvis. Acquired diseases such as Stones, Inflammatory diseases, Kidney masses, renal hypertension, renal obstruction and Vesicorectal.

Most of this disease affects the size of the kidney, while other may likely to change in the renal tissue i.e. (cortex, medulla and pelviocalyceal system) (Mark H and Beers, 2010).

2-4 Diagnosis :

During the physical examination for a suspected kidney or urinary tract disorder, doctor tries to feel the kidneys. Normally kidney can't be felt, but swollen kidneys or a kidney tumor may be detectable. Additional procedures to diagnose disorders of the kidneys and urinary tract may include urine analysis, blood tests, that reflect kidney function. Imaging procedures, tissue and cell sampling. (Mark H, Beers M 2010).

2-4-1 Imaging procedures:

An x-ray of the abdomen can show the size and position of the kidneys and urinary tracts include:

- Plain KUB.
- Intravenous urography (I.V.U).
- Cystogram.
- Retrograde urography.

Ultrasound scanning uses sound waves to produce image of anatomic structures. The technique is simple, painless, and safe. Ultrasound scanning is an excellent way to estimate kidney size and to diagnose a number of kidney abnormalities.

Computer tomography (CT) is more expensive then ultrasound scanning and intravenous urography but has some advantage. Because CT scans can distinguish soil structures from those that contain liquids, they're most useful in evaluating the type and extent of kidney tumors or other masses distorting the normal urinary tract. A radiopaque substance can be injected intravenously to obtain more information.

Magnetic resonance imaging (MRI) can provide information about kidney structures that can't be obtained by other techniques. Addition MRI produces excellent pictures of blood vessels and structures around the kidneys, so that a wide variety of diagnoses can be made. (Mark H, Beers M 2010).

Kidney Magnetic Resonance Imaging:

The difference in water content of the cortex and medulla of the kidney provides good contrast between renal parenchyma compartments by MRI. On T1 weighted images the cortex returns a higher signal than the medulla, because the renal cortex has lower water content and therefore a shorter T1 relaxation time (Torres & Ros, 1999). The renal sinus fat is differentiated well by its high signal intensity, whereas the renal pelvis and calices may be seen outlined by the low signal intensity of urine. Distension allows higher depiction. The renal vessels are depicted as low intensity tubular structures on T1W images. The renal fascia compartments are often outlines as a low intensity line. On T2W images the corticomedullary boundaries are poorly differentiated. The same is true after the

injection of gadolinium unless dynamic scanning us used. Renal arteries and veins return a high signal on gradient echo sequences, and urine returns a high signal on heavily T2W images (Baumgartner et al, 1992).

2-5 Kidney measurements :

A number of investigators have reported reference values for renal length (Emammian, M.B et al, 1993 - Allan .P et al, 2001) and renal volume in healthy adults (Emammian, M.B et al, 1993 – bakker. J et al, 1999), as measured by ultrasonography. The ultrasonography method that is measure kidney volumes in 2D in nature, and is operator dependent, and uses the geometric assumptions about the shape of the kidney to estimate volumes. In contrast, computed tomography (CT) and magnetic resonance imaging (MRI) can acquire three-dimensional data and therefore, it can estimate organs volumes in the case of CT, need for ionizing radiation and contrast media limits its place as a routine noninvasive imaging method for measuring kidney volumes. Conversely, MRI has the benefit of acquiring true tomographic data along any direction, without the constraints of ionizing radiation and nephrotoxic contrast burden. Nevertheless, the literature contains few reports of renal dimensions as determined by MRI (bakker. J et al, 1999), furthermore, although CT and MRI can be used to measure renal volume accurately with voxel count-based methods (binkert C.A et al, 1999). These techniques present problems of radiation exposure, and toxicity associated with renal contrast agents (miletic. D et al, 1998).

MRI estimation of kidney volumes can be determined using different methods including the water displacement. Disc summation and other mathematical methods it should be noted that tomographic images of the kidneys that were acquired using MRI can provide reliable and consistent determinations of kidney

volume without the geometric assumption limitations that are inherent in other methods of measurements. the changes in the acquired spatial resolution of the imaging techniques from a coarse spatial resolution to fine spatial resolution did not have an appreciable effect on the mean kidney volume measured. This suggests that the spatial resolution that was used in routine patient studies is sufficient to measure the kidney volumes accurately, and does not introduce significant errors in volume calculations. (Muthupillai .C. et al, 2007).

2-6 Texture analysis :

Texture analysis for computer-aided diagnosis (CAD) in medical images has been studied in many disciplines including the diagnosis of breast cancer in mammograms (Sahiner .S et al, 1998 - Zhang. M et al, 1996), lung nodules in chest radiographs [6-8], osteoporosis in bone x-ray images (Lan. L et al, 2007-. Wilkie. J.et al, 2004), and abnormalities in kidney and liver (Lee G.N. et al, 2006-. Kim. D et al, 2004). Analysis is typically based on regions-of-interest (ROIs). In this essence there are a number of different definitions of texture, when applied to image data. All definitions have in common the fact that they describe texture as an attribute of an image window. Texture is one of the important characteristics used in characterizing objects or regions of interest; (M Haralick et al, 1979-1973) developed a set of statistical features for classifying pictorial images. Chevaillier and Ponvianne proposed a semi-automated method to segment internal structures from a DCE-MRI registered sequence. They segmented cortex, medulla, and pelvis regions using the k-means partitioning algorithm. Pixels were classified according to their intensity (Chevaillier .B et al, 2008). Marcuzzo and Masiero segmented kidneys using the Expectation Maximization (EM) algorithm. They proposed 5 different classification methods to distinguish normal kidneys from rejected kidneys. They used symmetry of two kidney images, shape, relative position,

boundaries, and radiopharmaceutical information in DRE-MRI. They used 20 training kidney subjects to build reference information for these classification methods. For shape information they averaged 20 left and 20 right kidneys and determined a reference mean shape for a normal kidney (Marcuzzo et al. 2007). Koh and Shen suggested a segmentation procedure based on a generated rectangular mask and edge information to overcome the problem that no prior information about location or appearance exists. They also used threshold values in segmentation step. However, organs in DRE-MRI have similar gray level information. Also cortex, medulla, and pelvis regions of kidneys have similar gray level value in some scans. Therefore, segmentation based on threshold will not work to segment cortex and medulla regions in their case (Koh. M. et al, 2006). Xie and Jiang proposed kidney segmentation from ultrasound images based on texture and shape priors. Texture features were obtained by applying Gabor filters on images through a two-sided convolution strategy (Xie. J. et al, 2005).

Segmentation of the kidney into classes using texture is a challenging task in respect to the classifier and the type of texture. Therefore there are a number of different definitions of texture, when applied to image data. All Definitions have in common the fact that they describe texture as an attribute of an image window. These attributes can represent spatially deterministic aspects of the Grey level, including its stochastic color distribution properties (wagner1999).Goal et al. (1984) defined texture as structure composed of a large number of more or Less ordered similar patterns without any one of these drawing special attention. A Pattern like a checkerboard is said to have a deterministic texture, having a regular or Non random texture. Conversely the structure might resemble noise as on a television Monitor screen, and such a texture is said to be stochastic or statistically based on random Fluctuations. The two major characteristics of textures are its

coarseness and Directionality, thus the two major texture analysis approaches are statistical and Structural.

Texture is one of the important characteristics used in characterizing objects or Regions of interest. Heraldic et al. (1973) and haralick (1979) developed a set of Statistical features for classifying pictorial images. The statistical features are based on A matrix derived from the spatial distribution of grey level values in the pixels of the Image. This matrix is known as the spatial grey level dependence (SGLD) matrix. The Sgld matrices describe how often pairs of pixels, which are separated by a certain Distance and lie along a certain direction, occur in a digital image with some texture .Generally sgld matrices are not used directly, but statistical quantities based on They are computed to describe the characteristics of the textures. Texture features, Also referred to as haralick features can be computed from the sgld matrix. Some Of these measures are related to specific textural characteristic of the image such as Homogeneity, contrast, greys level linear dependence, or complexity of the image .Even though these texture features contain information about the texture characteristic Of the image it is hard to identify which specific texture is represented by each of Those features. These textural measures include entropy, energy, inverse Difference moments, sum entropy, correlation, Difference average, sum variance, information measure of Correlation (1) and variance and are detailed in Section 4.

2-7 Feature selection:

A number of algorithms can be used to select the optimum subset of features, to avoid Redundancy and co-linearity between the features Tourassi et al (2001) used mutual information as a criterion for feature selection for a Non linear classifier. Mutual information selection criteria need a large data set and Also depend upon the number of histogram bins that are determined empirically. This Is thus a limited method of feature selection.

Walker et al. (2003) used genetic algorithms for texture feature selection. The basic Approach was to create a combination of randomly selected texture features. Each Combination was considered a possible solution. The main advantage of a genetic A number of algorithms can be used to select the optimum subset of features, to avoid Redundancy and co-linearity between the features.

Algorithm is its ability to investigate many possible solutions simultaneously. Although successful, genetic algorithms are computationally very demanding, particularly as the number of available features increases. Texture features have been used in medical imaging for many purposes, for example To classify and assess renal tissues in MR images.

2-8 previous study:

Glodny et al. (2009) stated that normal kidney size and its influencing factors - a 64-slice MDCT study of 1.040 asymptomatic patients". The kidney is approximately 11–14 cm in length, 6 cm wide and 4 cm thick. Each adult kidney weighs between 125 and 170 grams in males and between 115 and 155 grams in females] the left kidney is usually slightly larger than the right kidney.

Kiw-yong et al. (2006) described in a comparative study methods of estimating kidney length in kidney transplantation donors to determine the usefulness of body index and radiological measurements for prediction of kidney size. This study includes 125 live kidney donors were between 20 and 65 years of age. The mean age of donors was 37 years; 37 were males and 39 were females. Their weight ranged from 41 kg to 108 kg (mean = 63 kg) and their height ranged from 150 cm to 187 cm (mean = 166 cm). BSA ranged from 1.4 to 2.3 (mean = 1.7) and mean TBW was 35.6 ± 6.9 .The sizes of donor kidneys obtained after nephrectomies for kidney transplantations were documented and the correlation coefficient between kidney length and body index was calculated. Kidney length was estimated from the distance between the first and third lumbar vertebrae (L1-3), intravenous pyelograms (IVPs), abdominal ultrasonography (US), and abdominal computed tomography (CT). Their results showed Normal adult kidneys were 11.08 ± 0.96 cm long, 6.25 ± 0.67 cm wide, 4.73 ± 0.65 cm thick and weighed 196.3 ± 41.0 g. Correlation coefficients between kidney length and body height, body weight, body surface area and total body water content were 0.29, 0.31, 0.26, and 0.32, respectively. The difference between actual and predicted kidney lengths was −0.6 cm for L1-3,

+1.2 cm for IVPs, −0.7 cm for abdominal US, −0.8 cm for transverse CT section, and −0.5 cm for coronal CT section. The correlation coefficients between actual kidney length and height, weight, BSA and TBW were 0.29, 0.31, 0.26 and 0.32 respectively ($P < 0.05$; Table 3). The relationship between actual kidney length and body index, body height and body weight estimated from multiple regression was: kidney length (cm) = 7.968 + 0.01163 × body height (cm) + 0.01795 × body weight (kg) ($R2 = 0.294$, $F = 5.065$, $P = 0.008$). Glomerular filtration rate is also correlated with actual kidney length. Renal size estimated from intravenous pyelograms (IVPs), actual renal size and the line of equality ($r = 0.524$, $P < 0.001$). Renal size estimated from abdominal ultrasonography (US), actual renal size and the line of equality ($r = 0.582$, $P < 0.001$). Renal size estimated from transverse sections of abdominal computed tomography (CT), actual renal size and the line of equality ($r = 0.541$, $P < 0.001$). Renal size estimated from coronal section of abdominal computed tomography (CT), actual renal size and the line of equality ($r = 0.603$, $P < 0.001$).

Breau (2013) Used simple method to estimate renal volume from computed tomography to evaluate the accuracy of simple renal measurements and estimate renal volume as compared with estimates made using specialized CT volumetric software. this study in 28 patients with contrast-enhanced abdominal CT. Using a standardized technique, one urologist and one urology resident independently measured renal length, lateral diameter and anterior-posterior diameter. Using the ellipsoid method, the products of the linear measurements were compared to 3D

volume measurements made by a radiologist using specialized volumetric software. Linear kidney measurements were highly consistent between the urologist and the urology resident (interclass correlation coefficients: 0.97 for length, 0.96 for lateral diameter, and 0.90 for anterior-posterior diameter). Average renal volume was 170 (SD: 36) cm(3) using the ellipsoid method compared with 186 (SD 37) cm(3) using volumetric software, for a mean absolute bias of -15.2 (SD 15.0) cm(3) and a relative volume bias of -8.2% ($p < 0.001$). Thirty-one of 56 (55.3%) estimated volumes were within 10% of the 3D measured volume and 54 of 56 (96.4%) were within 30%.

Cheong B et al. (2007) determined Normal Values for Renal Length and Volume as Measured by Magnetic Resonance Imaging. The objective of this study was to (1) test the validity of the ellipsoid formula for estimating kidney volume using ex vivo and in vivo models and (2) establish a normal range of values for kidney length and volume in patients with no known history of renal disease. The volumes of five excised porcine kidneys were measured by (1) disc-summation method, (2) ellipsoid formula, and (3) water displacement method. In a retrospective, consecutive group of clinically referred patients (n = 150; 300 kidneys), individual kidney volume and length were calculated by the disc-summation method and by multiplanar reformation of MRI data, respectively. For comparison, kidney volumes also were calculated using the ellipsoid formula in all patients. This study includes 150 consecutive patients (89 women; 61 men) who had undergone abdominal MRI. Their results showed that the Renal volumes by disc-summation and ellipsoid

methods in men and women (mean ± 1 SD) There was a modest correlation between kidney length and volume in both men and women ($r = 0.5$ in men; $r = 0.6$ in women). There was no correlation between the kidney volumes and BSA in women. However, there was a modest correlation between kidney volume and BSA in men ($r = 0.5$). The kidney volumes that were calculated by the ellipsoid formula were significantly smaller in both genders ($P < 0.0001$) when they were compared with the MRI disc-summation method. The mean kidney volume was approximately 18% less by the ellipsoid method in men and 15% less in women.

Harmse et al. (2011) determined Normal variance in renal size in relation to body habitus. This study investigates this relationship in order to determine normal ranges in relation to body habitus. And to evaluate the relationship of renal size to gender and race. Kidney lengths were measured on oblique coronal reformatted CT images of 514 patients who received routine abdominal CT scans for conditions unrelated to renal pathology. The patients had normal serum creatinine levels, no history of renal disease, no renal masses, and normal-appearing kidneys on CT. Weight, height, race and gender of the patients were recorded. Result was demonstrated the mean renal length was 108 mm with a standard deviation of 9.82 mm. a relationship between kidney size and body weight and height, both individually and collectively. The most accurate prediction model was ‘kidney size = 49.18 + 0.21 x weight + 0.27 x height’, with a r2-value of 0.32. Additionally, kidneys were generally larger in the white population than in the black, and also in males than females.

Brandt et al. (1982) assessed normal renal dimensions using Ultrasound. Their study confirms that the accuracy and reliability of sonographic assessment of renal dimensions when meticulous scanning techniques are employed. Sonographic renal dimensions are smaller than those obtained by radiography, since there is neither the geometric magnification nor the change in size related to an osmotic dieresis from iodinated contrast material. Sonographically, with patients in the prone position, the mean right renal length was 10.74 cm (± 1.35 SD) and the mean left renal length was 11.10 cm (± 1.15 SD). A prospective sample demonstrated the mean depth (ventral-dorsal dimension) to be approximately 4.5 cm when the transducer was angulated for the lie of the kidney.

Shin et al. (2009) measured the Kidney Volume with Multi-Detector Computed Tomography Scanning in Young Korean to estimate the normal kidney volume of healthy young Korean men and evaluated its predictability of renal function and relationship with body indexes. Their study included 113 patient Images were obtained prior to and after the administration of 150 mL of iodinated contrast media during the parenchymal phases of enhancement. The kidney size was measured using GE Advantage Windows Workstation, and kidney length was measured using coronal sections. Maximum kidney length was calculated from all coronal sections. The kidney volume was measured from contiguous slices. In coronal section images with parenchymal enhancement, the region of interest was drawn around the kidney, and the slices were reconstructed at 1-mm intervals to obtain a 3-D volume-rendered image of the kidney. The volume was calculated by multiplying the sum of areas from each slice by the reconstruction interval at the

workstation. Their results showed that the mean kidney volume was 205.15 cm2 (138.53-359.6 cm2). The left kidney was significantly ($p < 0.05$) larger than the right kidney, and they were highly correlated (correlation coefficient: $r = 0.874$, $p < 0.05$). The mean kidney length was 108.02 cm (9.09-12.49 cm). The left kidney was also significantly ($p < 0.05$) longer than the right kidney. The kidney length and kidney volume were highly correlated reciprocally ($r = 0.671$, $p < 0.05$)

MRI in Kidney have spatial image resolution On T1 weighted images the cortex returns a higher signal than the medulla, because the renal cortex has lower water content and therefore a shorter T1 relaxation time (Torres & Ros, 1999). The renal sinus fat is differentiated well by its high signal intensity, whereas the renal pelvis and calices may be seen outlined by the low signal intensity of urine. Distension allows higher depiction. The renal vessels are depicted as low intensity tubular structures on T1W images. The renal fascia compartments are often outlines as a low intensity line. On T2W images the corticomedullary boundaries are poorly differentiated. The same is true after the injection of gadolinium unless dynamic scanning us used. Renal arteries and veins return a high signal on gradient echo sequences, and urine returns a high signal on heavily T2W images (Baumgartner et al, 1992).

Chapter three
Material and method

This is an analyze and experimental study focuses on the measure kidney volume and analysis of kidney tissues depicted by magnetic resonance image using DSM for measurements and using textural features properties to analyze the tissues , it is conducted at Khartoum state (Al amal Hospital) in period June 2012 and June 2013.

3-1 Material:

- ✓ **(**MRI machine – Philips, Intrea MRI system magnetic felid strength 1.5 tesla. Software version: 3.2.1/1.2.3.
- ✓ Metric scale for patient's heights.
- ✓ Weight scale, in (KG) s.

3-1-1 sample size:

One hundred normal adults male and female at the age of (20-45) years old. Come to hospital to Al- amal hospital – diagnostic department to do L/S exam in MRI. Detailed demographic information of the population including age, gender, weight, and high, BMI, BSA, TBW, SrCr, CrCl, and GFR was recorded.

Include criteria:

Ninety-eight consecutive patients (43 female; 55 males) their ages were between 20 – 45 years who had undergone axial T1,T2 abdominal MRI weighted images for indications other then renal disease .

Excluding criteria:

Patients were those who had renal cysts, hydronephrosis, and congenital kidney disease.

3-1-2 data analyze:

The data was analyzed by a PC dell inspion 2.1 GHz using Interactive Data Language (IDL) Version 6.1(http://www.ResearchSystems.com) . IDL is a complete structured language that can be used to create sophisticated functions, procedures and applications. It is an efficient Programming tool for Image processing and is available for most computer plat forms and enables rapid implementation of algorithms and is a convenient image processing Development tool. As well as SPSS version 21 and excel where classification coefficient will be developed to classify and unseen images into three classes. The accuracy of the classifier and specificity and sensitivity will be checked. and also used these programs to be used in the measurements of the kidneys, which will be separated later.

3-2 Method:

3-2-1 Technique of data collection:

MRI Protocol:

MRI machine 1.5 Tesla was used at AL-amal hospital, the selected sequences were Scout: axial sagittal, and coronal. Sequence 1 and 2 were coronal and axial T2-

weighted: TSE, breath hold: TR=3000-4000, TE=90-140, respiratory triggering TR=1900-2300, TE=100, Flip angle 90oSTIR: TR= 2200, TE =60, TI=100 HASTE, breath hold; TR =11.9, TE= 95, Slice thickness 4-6 mm. Slice gap : (0.8-1.2mm),phase encoding gradient: LR,FOV : 380-400mm, sequence 3 was axial T1-weighted, GRE (FFE), breath hold: TR = 120-140,TE= 4 Flip angle 60oGRE (FFE), respiratory compensation : TR=500-600, TE=10 or as SPIR : TR =500-600, TE=15, or TSE, breath hold: TR = 320, TE=14, Matrix = 140x256.

Method of kidneys length and volume measurements:

Disk summation method (DSM) was used to calculate the volume of normal kidney in normal individuals. In the DSM, the measurement is dependent on the picture element (pixel-px), by counting the total number of px per unit area (only renal area excluding the rest of FOV, and is represented in (px^2). Then the px are converted into units of area in (mm^2).that is done by multiplying the area in (px^2) by conversion constant $(0.26)^2$,

Then multiplying the product by slice thickness in (mm),which represents slice height an Z-axis ,and consequently the product is in unit volume (mm^3) for the single slice. Then dividing the value in (mm^3) over (1000) to convert it to (cm^3). This formula is applied to each separate to final the total volume of both kidneys as shown in following equations:

- Px^2 (number of pixels)^2 x $(0.26)^2$=Area in $(mm)^2$ Eq (1)
- Area $(mm)^2$ x slice thickness (mm) = volume $(mm)^3$ Eq (2)
- Volume $(mm)^3/1000$ = volume $(cm)^3$ Eq (3)
- Total volume of kidney = ∑slices volumes. Eq (4)

Also three measurement are calculated to determine the (complete volume) which is are assumption that kidney is degrader (regular shape) which is the product of multiplying three damnation length z-axis x width x-axis x depth y-axis .To

determine the length which is represented by unit distance in the z-axis according to patient's position inside the gantry of MRI, and can be expressed by slice thickness, and is calculated by:

- Length = number of slices (in which kidney appeared) x slice thickness (cm) Eq (5)

The width which is also represented in unit length in the x-axis, and calculated by the cube root of volume (cm) ^{3}

- Width (cm) $=\sqrt[3]{\text{total volume (cm)}^3}$. Eq (6)

The depth in unit length on the y-axis calculated by, dividing the square root largest area calculated in $(mm)^2$ over 10.

- Thickness (cm) $=\sqrt{largest\,area\ (mm)}2/10$ Eq (7).

After determine the 3 dimensions above, the assumed renal volume can be calculated based on the mathematical rule:

- Volume $(cm)^3$= length x depth x width. Eq (8)

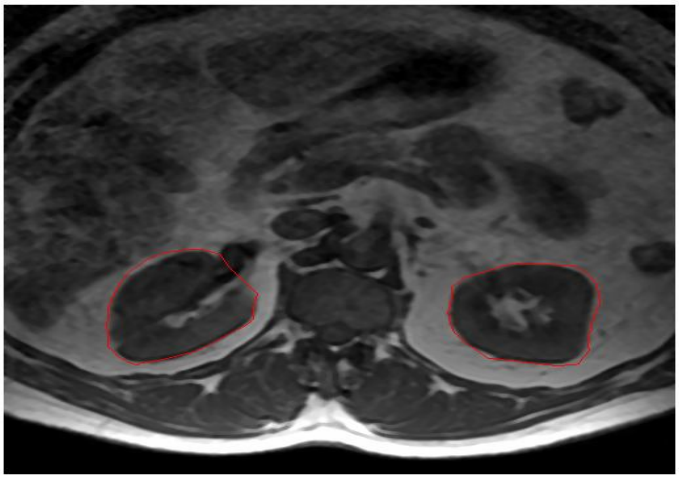

Fig (3-1) kidney contouring in one slices T_1 TSE MRI.

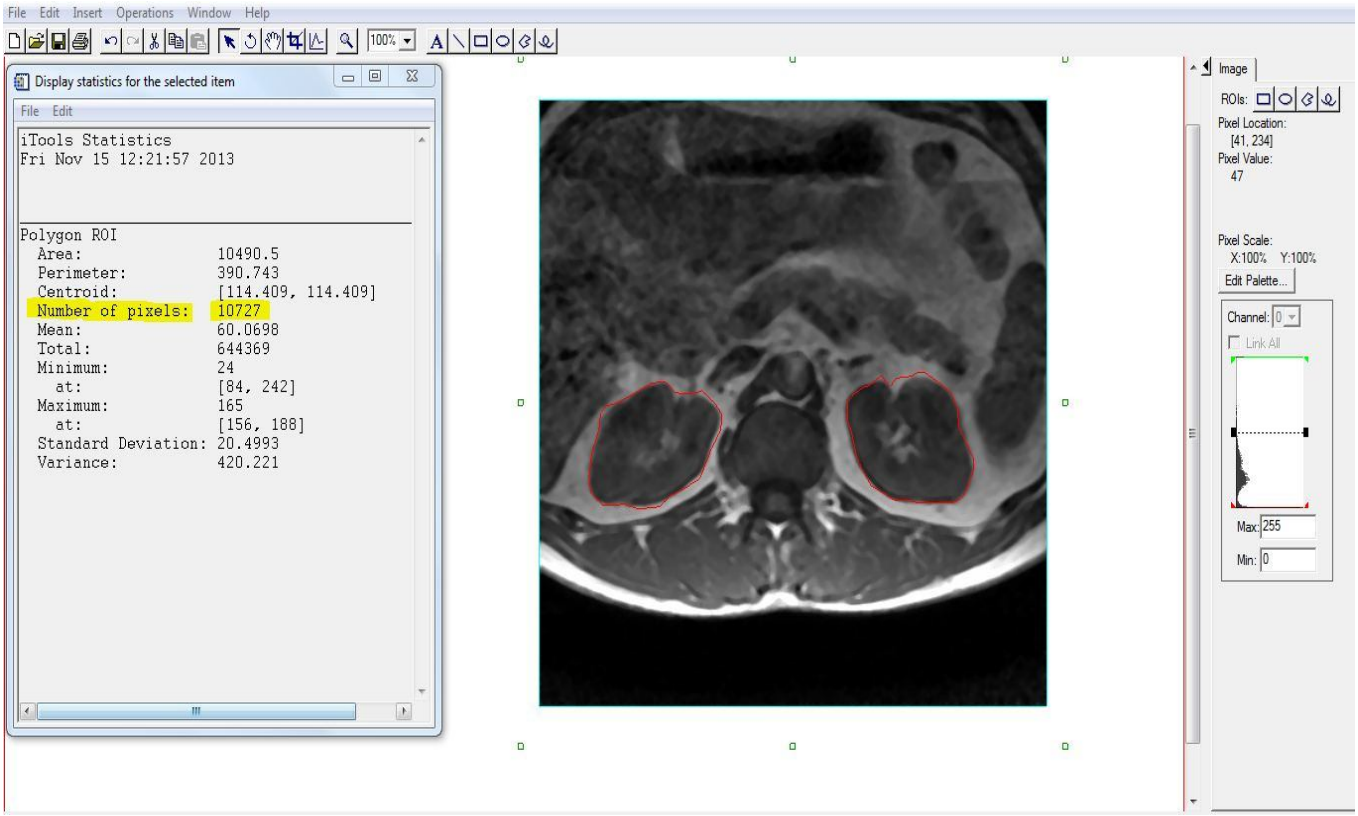

Fig (3-2) number of pixel collection.

Methods of variables evaluation:

Independent variables: height; which measured in (cm).weight in (kg), age in (yrs) and gender (male or female) were evaluated. For measuring dependent variables:

- Body surface area (BSA), in $(m)^2$ total body water (TBW) in (liters) and Glomerular filtration rate (GFR) by (Cock–Craft-Gault) (CG) equation in $(ml/min/1.73.mm^2)$.
- To calculate BSA in $(m)^2$ (Gehan .E.- 1970).

{(height (cm)) x (weight (kg)) /3600} x1/2 Eq (9)

- Total body water is calculated by Watson's formula(Watson .P.-1980):

- TWB_{male} = (2.477-0.09516 x age (yrs) +0.1074 x height (cm) +0.3362 x weight (Kg)
- TBW_{female} = (-2.097+ (0.106) x height (cm)+0.2466 x weight (kg). Eq (10.11)

- To determine (GFR) ,we use the CG-GFR equation(Cockcroft.D.-1976) :

- CrCl X BSA / 1.73$(m)^2$=GFR Eq 12)

When:

- (CrCl) Ceriatinine clearance = (140-age) x weight (kg) x {0.85 if female} /72Xserum Ceriatinine.
- Serum Ceriatinine in Sudanese population = (BMI*0.031) + (age*0.003) + (Gender*-0.52).

Method extracted textural feature:

The MRI images used in this study were selected randomly from the patient visited the department of Radiology, in Al-Amal Hospital. The sample size consisted of 100 abdominal MRI images of normal kidneys for male and female their age ranged from 20-40 years old normal MRI. The data was extracted from each of the images by using a windows of 5×5, 10×10, 15×15 and 20×20 pixels; where the data were extracted from a region of interest (ROI) that represent cortex, medulla and pelvic system of the kidneys. The co-occurrence matrix was generated as a function using IDL software for all windows and hence SGLD features (S. Poonguzhali, G. Ravindran – (2008) were computed using distance one and angle zero (θ°). A classification technique was applied in to classify the sub-images into three classes. Each feature victor was labeled according to the class of the ROI. Then discriminate analysis using the stepwise method was used to select the most discriminate feature and hence classifying the extracted feature into one of the labeled classes. The labels of each class were used as ground truth to account for the classification accuracy.

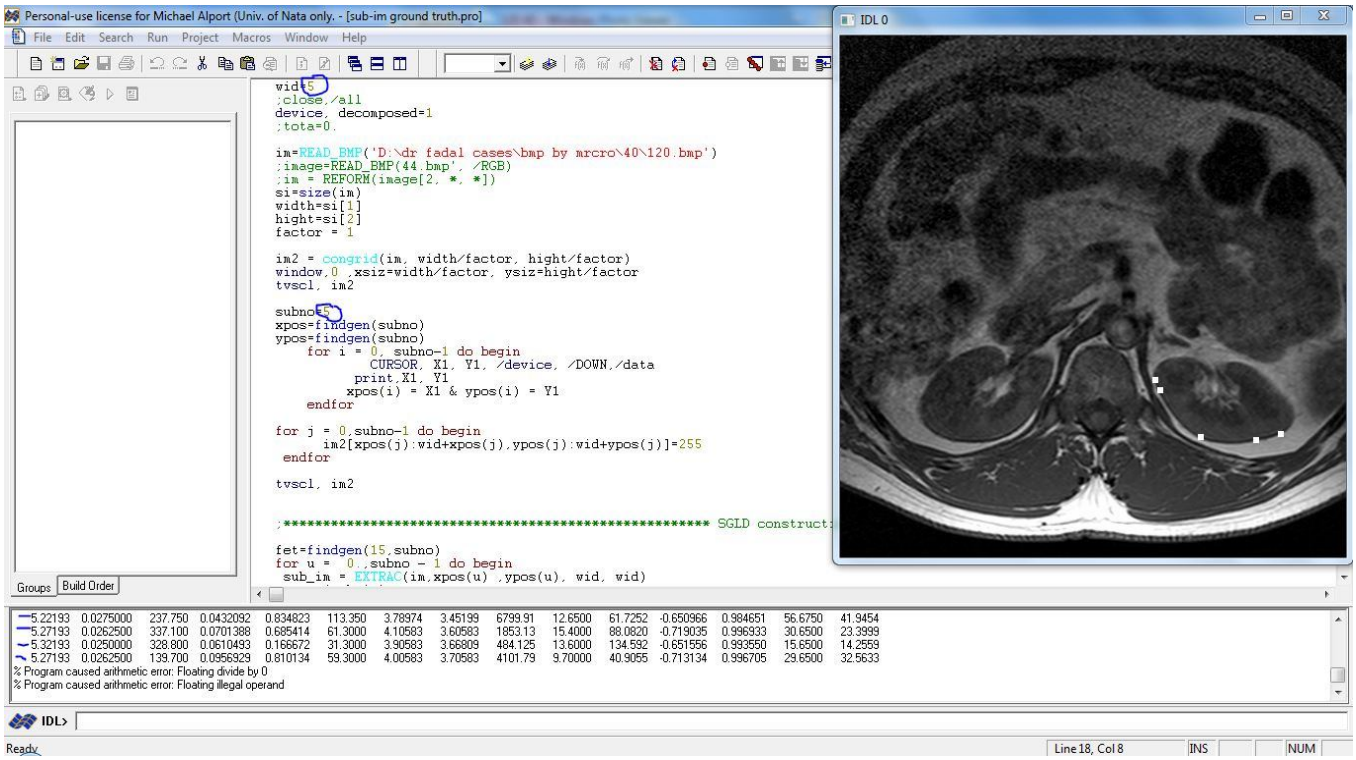

Fig (3-3) feature extraction from cortex when window size 5x5 pixel.

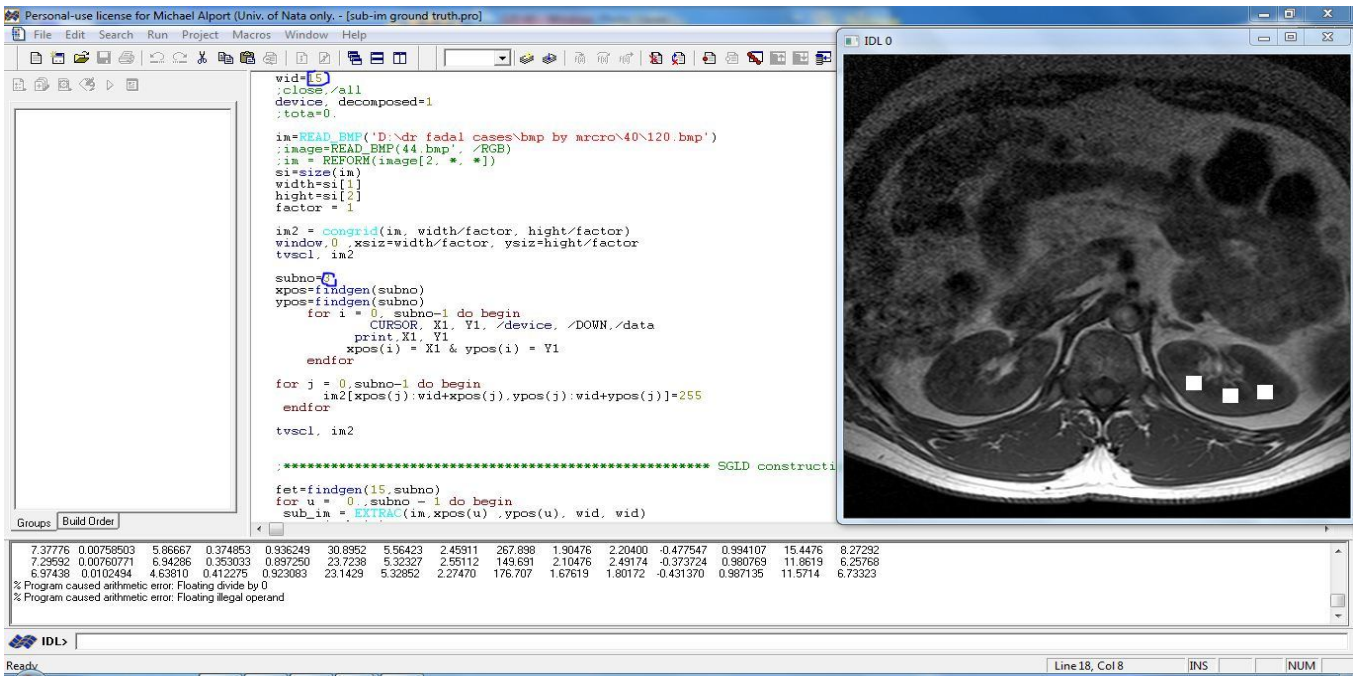

Fig (3-4) feature extraction from medulla when window size 15x15 pixels.

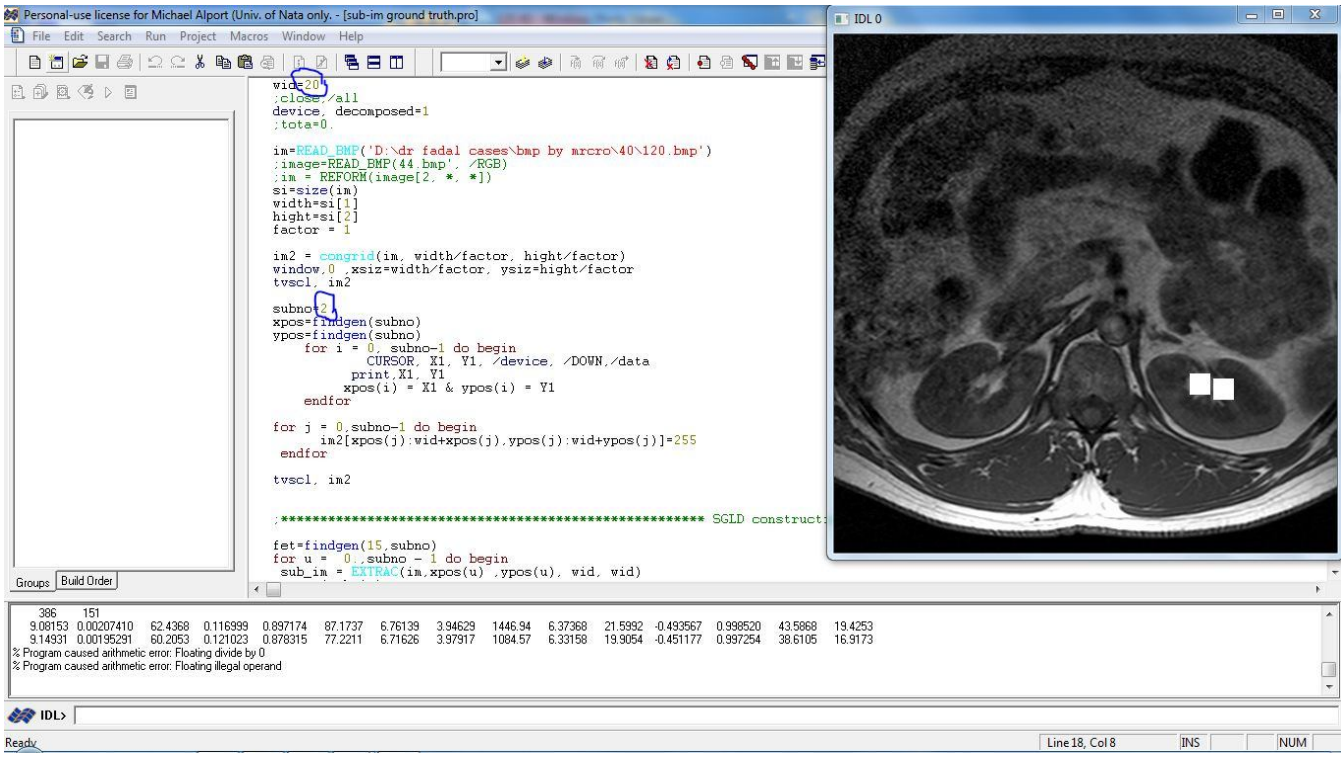

Fig (3-5) feature extraction from P/C system when window size 20x20 pixels.

3-3 Spatial Gray level dependence (SGLD) matrix:

The SGLD matrix, also known as the co-occurrence matrix, (as described by Haralick et al. (1979) uses second order statistics to characterize the relationships between nearby pixels within a region. The matrix size depends on the grey level resolution of the digitized mammogram. If the matrix was computed from a 14-bit image, with a bin width of 1 grey level, the matrix size would be 16384×16384 elements. The matrix size would be reduced to 256×256 elements if the grey level resolution is reduced to 8-bit. It has been shown that texture features computed from the SGLD matrix using 8-bit grey level resolution image provides better classification accuracy when texture features calculated at a fixed pixel distance *d* were used (Wei et al. 1995).

The (i, j)-th element of the SGLD matrix, $p_{d,\theta}(i, j)$, is the joint probability of occurrence of grey levels, i and j, for two pixels which are separated by a distance, d, and located along a line oriented at an angle θ. The values of the probability density functions will be denoted by $P_{d,\theta}(i, j)$. Formally, for angles quantized at 45° intervals the joint probability density functions are defined for an L_x by L_y matrix (Haralick et al. 1979) by:

$$P_{d,0^\circ}(i, j) = \#\{((k, l), (m, n)) \in (L_x, L_y) \times (L_x, L_y)$$

$$k - m = 0, \quad | l - n | = d,$$

$$I(k,l) = i, \quad I(m,n) = j\} \qquad \text{Eq (14)}$$

$$P_{d,45^\circ}(i,j) = \#\{((k,l),(m,n)) \in (L_x, L_y) \times (L_x, L_y)$$

$$(k - m = d, \quad l - n = -d)$$

$$\text{or } (k - m = -d, \quad l - n = d),$$

$$I(k,l) = i, \quad I(m,n) = j\} \qquad \text{Eq (15)}$$

$$P_{d,90^\circ}(i,j) = \#\{((k,l),(m,n)) \in (L_x, L_y) \times (L_x, L_y)$$

$$|k - m| = d, \quad l - n = 0,$$

$$I(k,l) = i, \quad I(m,n) = j\} \qquad \text{Eq (16)}$$

$$P_{d,135^\circ}(i,j) = \#\{((k,i),(m,n)) \in (L_x, L_y) \times (L_x, L_y)$$

$$(k - m = d, \quad l - n = d)$$

$$\text{or } (k - m = -d, \quad l - n = -d)$$

$$I(k,l) = i, \quad I(m,n) = j\} \qquad \text{Eq (17)}$$

Where # denotes the number of elements in the set, L_x and L_y are the horizontal and vertical spatial domain and $I(x, y)$ is the image intensity at point (x, y). These matrices are symmetric; $p_{d,\theta}(i, j) = p_{d,\theta}(j, i)$. The SGLDs are normalized by dividing each entry of the matrices by the total number of pairs as follows:

$$p(i, j) = \frac{P(i, j)}{n} \qquad \text{Eq (18)}$$

where $p(i, j)$ is the normalized SGLD matrix, $P(i, j)$ the un-normalized SGLD matrix, and n is the normalization factor, which is equal to the total number of pairs.

An example of the SGLD matrix calculation can be found in Section 3.4.1. Texture features, F_k, can be measured using SGLD matrix derived quantities, known as Haralick's texture features by summing each normalized SGLD matrix element multiplied by a weighting function, $W_k(i, j)$, the function were different for the different features as shown in Table 3-1, generally the features can be calculated as follows:

$$F_k = \sum_{i=0}^{n-1} \sum_{j=0}^{n-1} W_k(i, j) \times p_{d,\theta}(i, j) \qquad \text{Eq (18)}$$

Table **Error! No text of specified style in document.**-1 The mathematical description of the SGLD textural features, F_k.

Texture features	**Equation**
Energy (EG)	$$EG = \sum_{i=0}^{n-1}\sum_{j=0}^{n-1} p^2(i,j)$$ where n is the number of grey levels in the image.
Entropy (EN)	$$EN = -\sum_{i=0}^{n-1}\sum_{j=0}^{n-1} p(i,j)\log_2 p(i,j)$$
Inertia (IN)	$$IN = -\sum_{i=0}^{n-1}\sum_{j=0}^{n-1} (i-j)^2 p(i,j)$$
Inverse difference moments (IDM)	$$IDM = -\sum_{i=0}^{n-1}\sum_{j=0}^{n-1} \frac{1}{1+(i-j)^2} p(i,j)$$
Sum average (SA)	$$SA = \sum_{k=0}^{2n-2} k p_{x+y}(k)$$ **where,** $$p_{x+y}(k) = \sum_{i=0}^{n-1}\sum_{j=0}^{n-1} p(i,j),$$ $$i + j = k, \qquad k = 0,...2n-2$$
Sum entropy (SE)	$$SE = -\sum_{k=0}^{2n-2} p_{x+y}(k)\log_2 p_{x+y}(k)$$

Sum variance (SV)	$$SV = \sum_{k=0}^{2n-2} (k - SA)^2 \, p_{x+y}(k)$$
Difference average (DA)	$$DA = \sum_{k=0}^{n-1} k p_{x-y}(k)$$
Difference variance (DV)	$$DV = \sum_{k=0}^{n-1} (k - DA)^2 \, p_{x-y}(k)$$
Information measures of correlation1 (IMC1)	$$IMC_1 = \frac{EN - H_1}{\max\{H_X, H_Y\}}$$ **where** $$H_1 = -\sum_{i=0}^{n-1}\sum_{j=0}^{n-1} p(i,j) \log_2 \left[p_x(i) p_y(j) \right]$$ $$H_X = -\sum_{i=0}^{n-1} p_x(i) \log_2 \left[p_x(i) \right]$$ $$H_Y = -\sum_{j=0}^{n-1} p_y(i) \log_2 \left[p_y(j) \right]$$
Information measures of correlation2 (IMC2)	$$IMC_2 = \sqrt{1 - \exp\left[-2(H_2 - EN)\right]}$$ $$H_2 = -\sum_{i=0}^{n-1}\sum_{j=0}^{n-1} p_x(i) p_y(j) \log_2 \left[p_x(i) p_y(j) \right]$$ **where**
Variance (VA)	$$VA = \sum_{i=0}^{n-1} (i - \mu_x)^2 \, p_x(i)$$

Table (3-1) Texture Feature Equations

The texture features computed from the SGLD matrices can be categorized into four groups (Gool et al. 1984) as follows:

a) Features that express visual texture characteristics include:
    i) inertia (also known as homogeneity) (IN)
    ii) energy (also known as contrast) (EG)
b) Features that are based on statistics include:
    i) variance (VA)
    ii) inverse difference moment (IDM)
    iii) sum variance (SV)
    iv) sum average (SA)
    v) difference average (DA)
    vi) difference variance (DV)
c) Features that are based on correlation include:
    i) correlation (CO)
    ii) information measure of correlation$_1$ (IMC_1)
    iii) information measure of correlation$_2$ (IMC_2)
d) Features that are based on information theory include:
    i) entropy (EN)
    ii) sum entropy (SE)
    iii) Difference entropy (DE).

3-3-1 Classification technique:

The classification technique was used to characterize the normal kidney tissue in the magnetic resonance images into 3 classes, cortex, medulla, pelviocalyceal system. The input texture features were textures computed from the Spatial grey level dependence matrix (SGLD), which uses a statistical calculation of the spatial distribution of nearby pixels (as discussed in more details in Section 4).. A linear discriminate analysis using stepwise were used to classify the sample into the predefined classes. The stepwise method selected 9 features out of fifteen features as the most discriminate features; they included: Entropy (EN), energy (EG), inverse difference moment (IDM), sum entropy (SE), correlation (CO), sum variance (SV), and difference average (DA), information measures of correlation1and variance (VA). of 99 magnetic resonance images, were extracted using a moving window. a number of windows were used in 4 trials : (5x5)px ,(10x10)px ,(15x15)px and (20x20)px, in order was initially used, . Each texture feature was calculated at angles q = 0ºand at a distance, d = 1. The textural features from the ROI were classified using the K-means classifier into three classes (more detail is given in Section.4), normal, fatty and cirrhosis. The class centres obtained from these sub-images were used to classify unseen images according to their

minimum distance from the class centers. To classify the unseen images, textural features were first computed from the SGLD matrices for all images using a window of 80´80 pixels (more detail is given in chapter 4). The extracting window was incrementally moved in 20 pixels Steps on the, *x* an directions and at each step the texture features were calculated. In this way, The calculated features were then classified according to the minimum distance from the obtained class centers. Then a classification map for each image was constructed, and used to construct the confusion matrixes. The impact of co linearity on the classification accuracy was also Investigated using the correlation coefficient as a measure. The correlation coefficient matrix was generated by calculating the correlation between the features values that Were used as ground truth . .

3-3-2 Linear discriminate analysis:

Linear discriminate analysis (Ld) as described by Hair et al. (1998) is a statistical technique used to classify samples into one of a set of predefined classes. Therefore, Ld involves finding a linear combination of two (or more) features that will discriminate between the classes. The discriminate is found by setting weights for each feature that can maximize the "between class variance", (S_B) relative to the "within class variance", (S_W).

To compute, S_W, for d-dimensional features, F, we have to compute the mean, m, for each feature in each class as follows:

$$m_{ij} = \frac{1}{b_i}\sum_{p=1}^{b_i} F_{ij_p} \qquad \text{Eq (19)}$$

where m_{ij} is the matrix containing the means of the jth feature for the ith class

$i = 1, 2 \ldots K$, with K being the number of classes

$j = 1, 2 \ldots n$, with n being the number of features

$p = 1, 2 .. b_i$, with b_i being the number of elements in the ith class

Therefore the within class variance matrix is given by:

$$S_W = \sum_{i=1}^{K}\sum_{j=1}^{n}\left(F_{ij} - m_{ij}\right)\left(F_{ij} - m_{ij}\right)^T \qquad \text{Eq (20)}$$

To compute the "between class variance" matrix, first the grand mean, gm, should be computed as follows:

$$gm_j = \frac{1}{K}\sum_{i=1}^{K} m_{ij} \qquad \text{Eq (21)}$$

where gm_j is the grand mean for the jth feature.

$j = 1, 2 \ldots n$ with n being the number of features.

$i = 1, 2 \ldots K$ with κ being the number of classes.

m_{ij} is a matrix containing the mean of the jth features for the ith class.

Then the between class variance matrix is given by:

$$S_B = \sum_{i=1}^{K} (m_{ij} - mg_j)(m_{ji} - mg_j)^T \qquad \text{Eq (22)}$$

3-3-3 Classification function*:*

Discriminate analysis provides a basis for classifying not only the sample used to compute the discriminate function, but also any other observations that can have value for all the features by generating a *classification function*. In this way, discriminate analysis can be used to classify other features into defined classes. The number of classification functions is equal to the number of classes. Each function allows the computation of a classification score for each feature by applying an equation, which takes the following form:

$$S_i = a_i + \sum_{j=1}^{n} W_{ij} \times F_j \qquad \text{Eq (23)}$$

Where S_i is the resultant classification score for the i^{th} class,

$i = 1, 2, 3 \ldots K$ with K being the numbers of classes,

q is a constant for the $_i{}^{th}$ class,

$W_{i,j}$ is a weight function for the j^{th} feature for the $_i{}^{th}$ class,

$j = 1, 2, 3...n$ with $_n$ being the number of features.

F_j denotes the value of the j^{th} features.

Thus, a classification is achieved by multiplying each feature for an individual case by its corresponding weight in the different classes and adding these products together in each class. This process results in a single classification score for each class. Once the classification score is computed, the case is thus classified as belonging to the class in which it has achieved the highest score, and the process is continued in the same fashion for the rest of the features. The function, W, and the constant, $_a$, can be computed as follows: (Dillon and Goldstein 1984, Johnson and Wichern 1992):

$$W_i = S_p^{-1}(m_{ij})^T \qquad \text{Eq (24)}$$

where S_p^{-1} is the invert of between class variance which is given by:

$$S_p = \frac{S_B}{\left(\sum_{i=1}^{K} n_i\right) - K} \qquad \text{Eq (25)}$$

The constant $_a$ is given by:

$$a_i = \frac{1}{2}\sum_{i=1}^{K}(m_i)^T S_p^{-1} m_i \qquad \text{Eq (26)}$$

Chapter four
Result

The result of this study presented in tables and figures illustrate the relationships between all the variables in this study.

Table (4.1): descriptive statistics of the normal Sudanese body characteristics (total sample):

	Range	*Mean ± SD*	*Normal range*
Weight (kg)	66-101	83.4±8.2	==
Age (yrs)	20-45	32.0± 6.1	==
Body surface area (BSA)	1.55-2.50	2.04±0.20	1.39-2.60m2
Body mass index (BMI)	21.10-34.95	26.81±3.20	21.97-22.48 male & female
Height (cm)	164-186	176.0±4.49	==
Total body water (TBW)(L)	33.20-52.64	42.76±5.49	30-55
Serum Ceriatinine (SrCr)	0.67-1.15	0.8±0.10	0.5-1.5
Ceriatinine clearance (CrCl)(mg/dL)	62.62-161.51	99.36±21.76	99.36±21.76
Cockcroft -Gault Glomerular filtration rate (CG-GFR) (ml/min/1.73m2).	56.07-222.64	119.0±37.08	50-250

Table (4. 2): descriptive statistics mean standard deviation of kidneys volume, and length for the total sample

	Range	Mean ± SD
Right kidney volume (cm3)	80.32-122.91	101.6±12.98
Right kidney length (cm)	9-11.25	10.18±0.46
left kidney volume (cm3)	82.56-126.54	104.0±12.99
Left kidney length (cm)	9-11.70	10.67±0.47

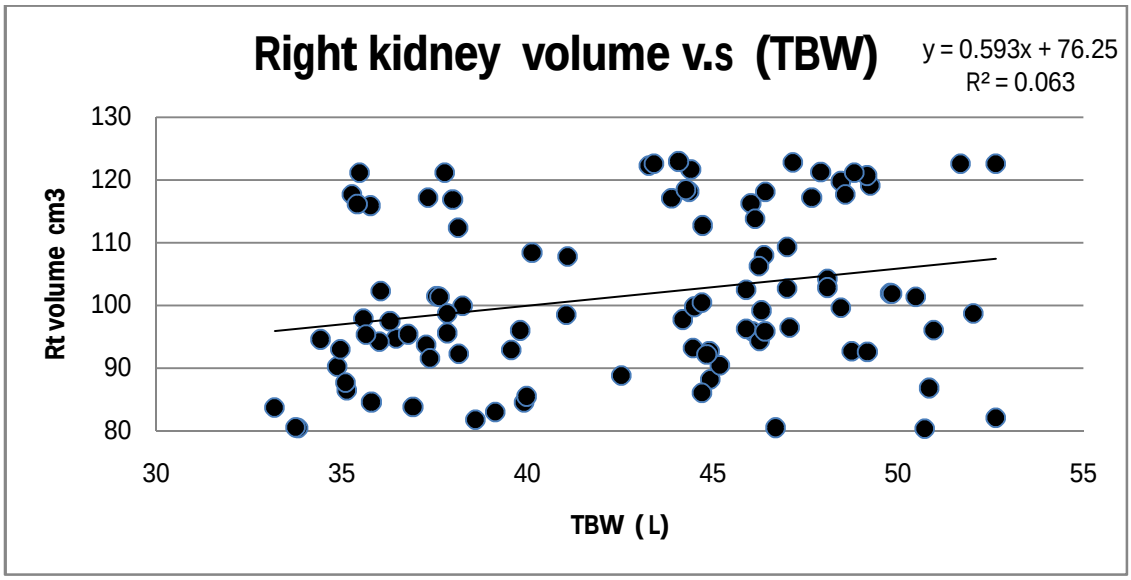

Fig (4.1): scatter plot diagram showed a linear relationship between the total body water (TBW) and RT kidney volume with a significant correlation (*p*= 0.013)

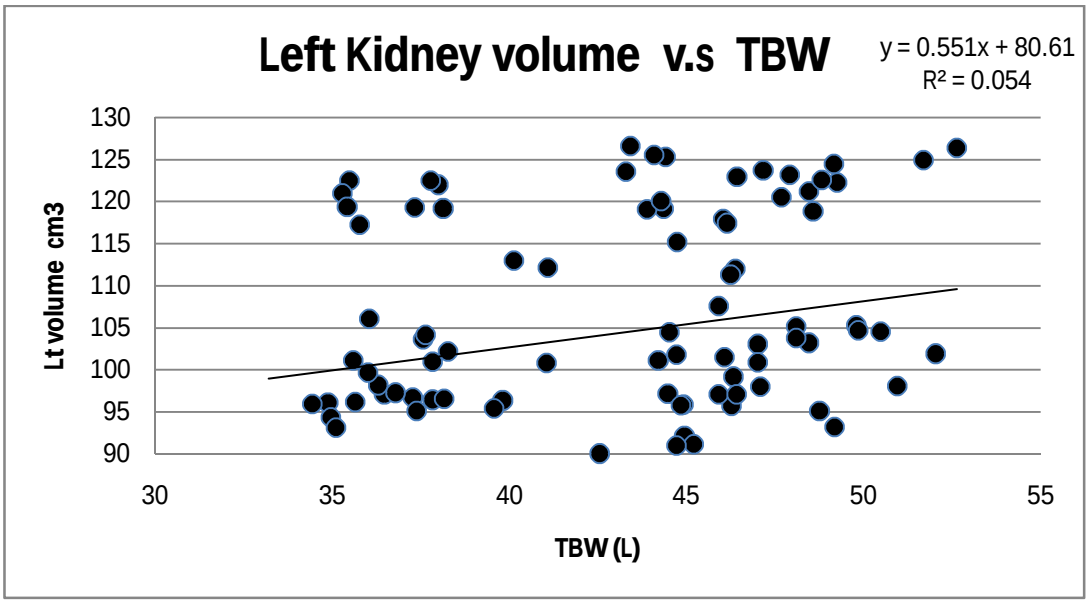

Fig (4.2): scatter plot diagram showed a linear relationship between the total body water (TBW) and LT kidney volume with a significant correlation (*p*=0.021)

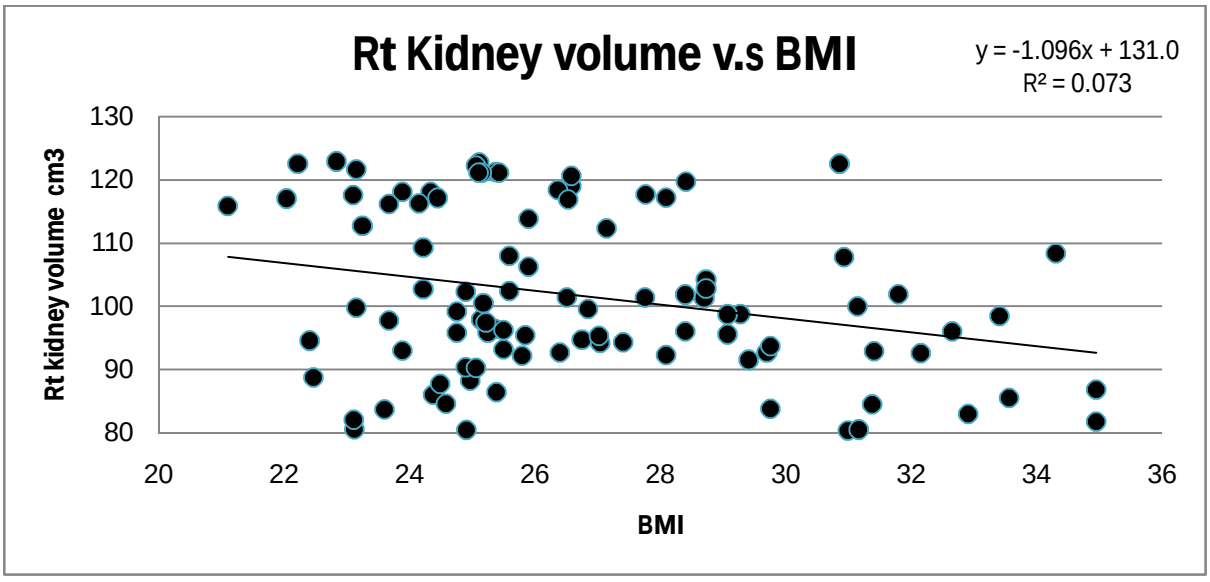

Fig (4.3): scatter plot diagram showed a linear relationship between the Body mass index (BMI) and RT kidney volume with significant correlation (*p*=0.007)

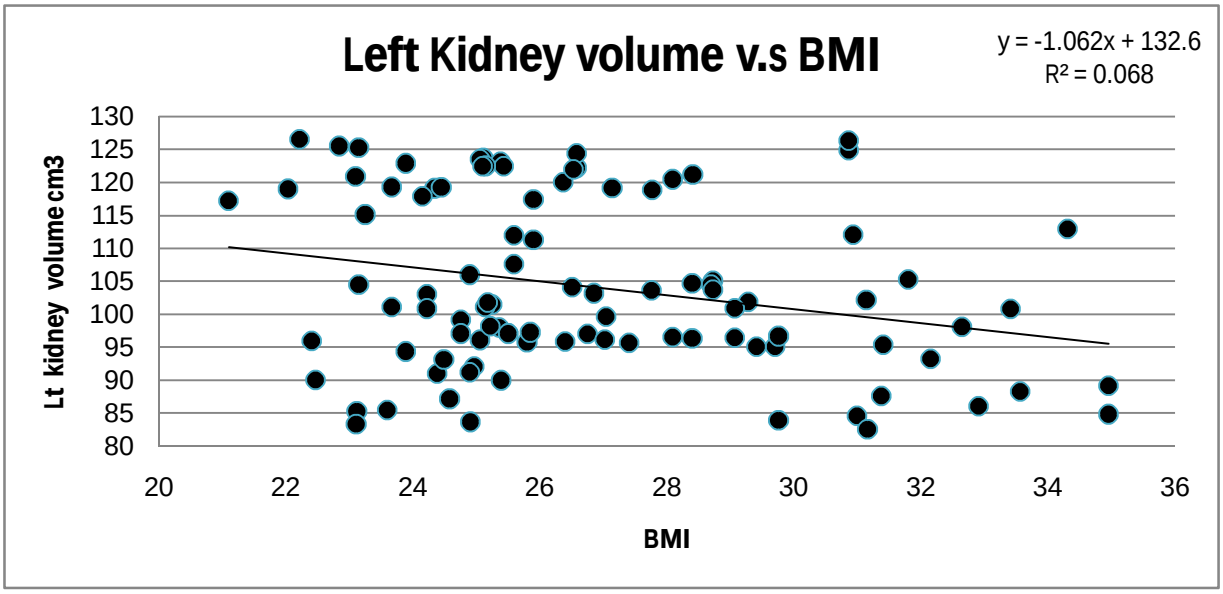

Fig (4.4): scatter plot diagram showed a linear relationship between the Body mass index (BMI) and RT kidney volume with a significant correlation (*p*=0.009)

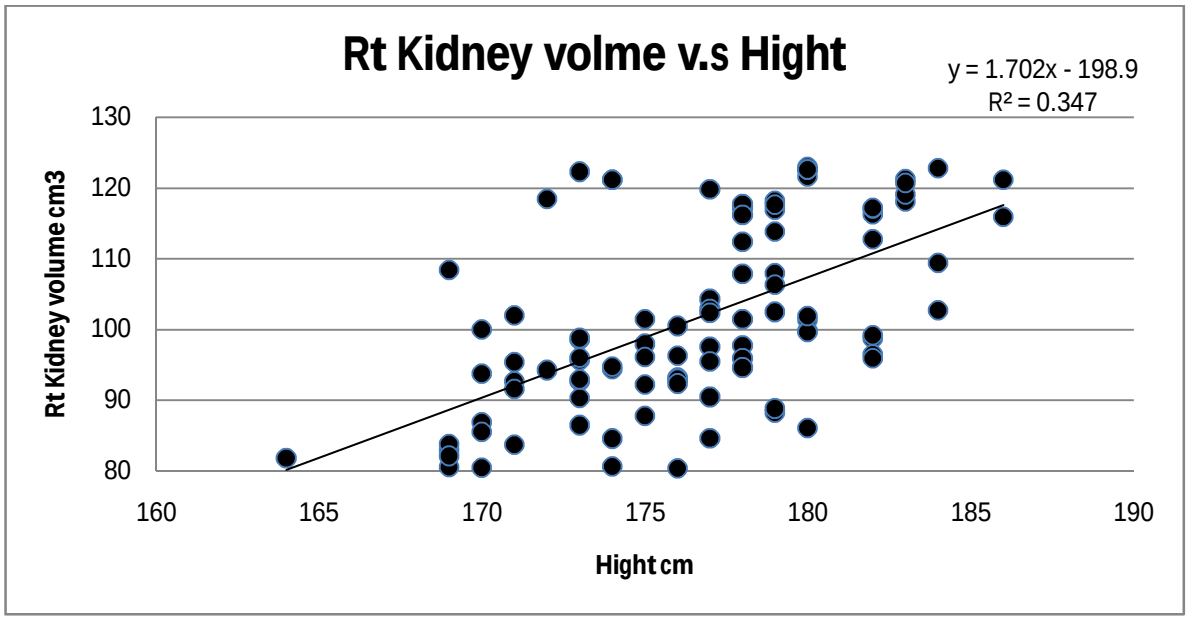

Fig (4.5): scatter plot diagram showed a linear relationship between the Height and RT kidney volume with a significant correlation (*p*=0.000).

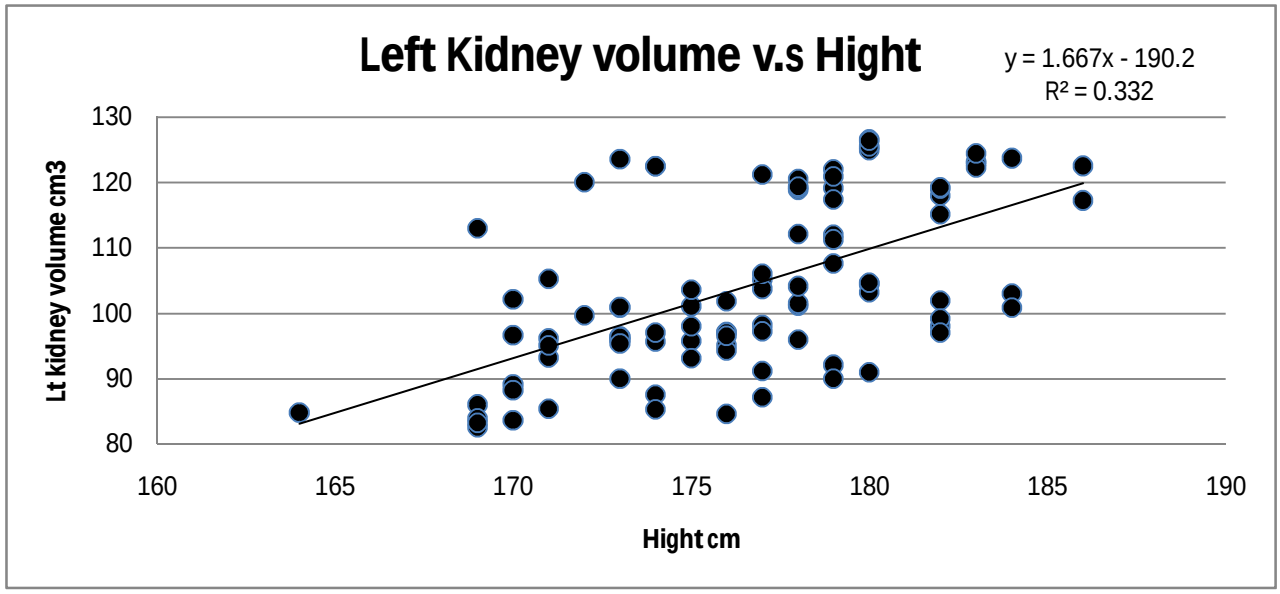

Fig (4.6): scatter plot diagram showed a linear relationship between the Height and RT kidney volume with a significant correlation (*p*=0.000).

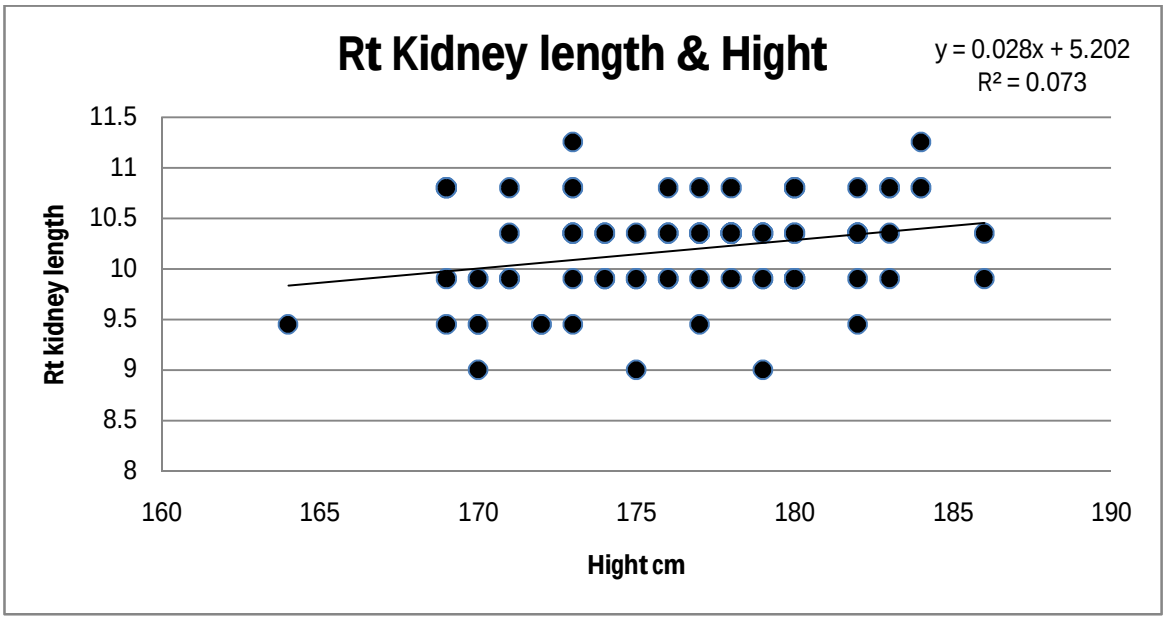

Fig (4.7): scatter plot diagram showed a linear relationship between the Height and RT kidney length with a significant correlation (*p*=0.007).

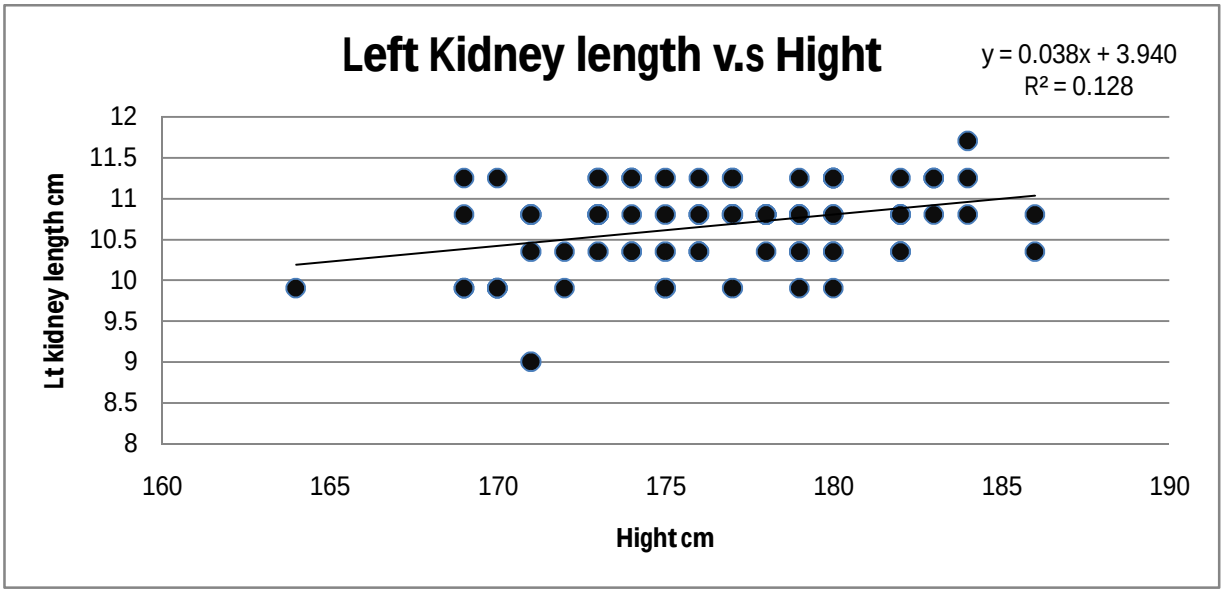

Fig (4.8): scatter plot diagram showed a linear relationship between the Height and LT kidney length with a significant correlation (*p*=0.000) .

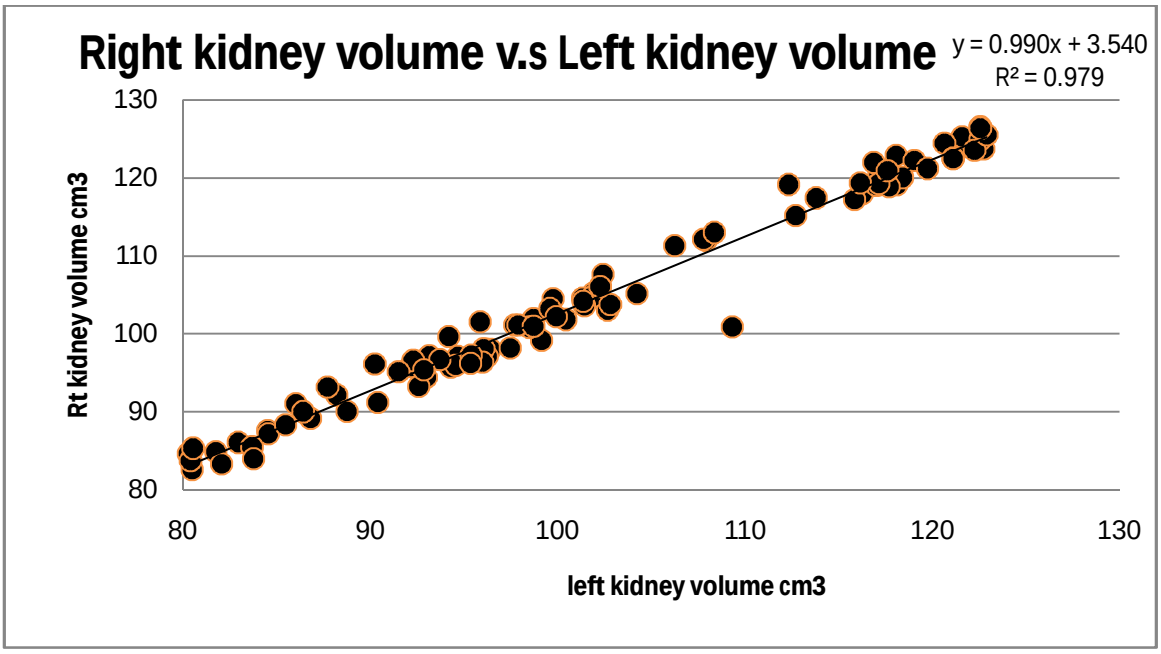

Fig (4.9): scatter plot diagram showed a linear relationship between the LT kidney volume and RT kidney volume with a significant correlation (*p*=0.003)

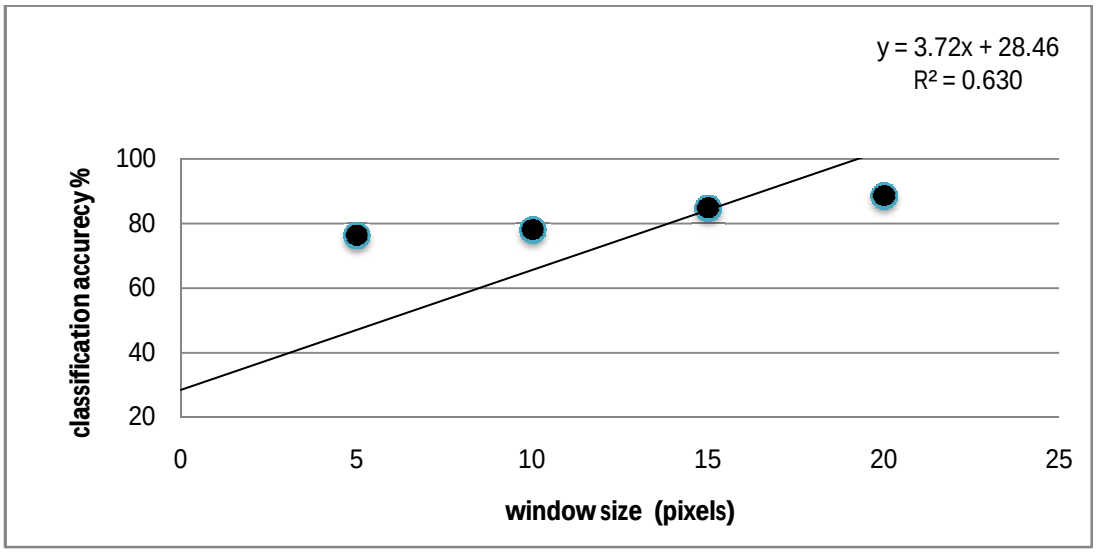

Fig (4.10) Classification accuracy versus window size .

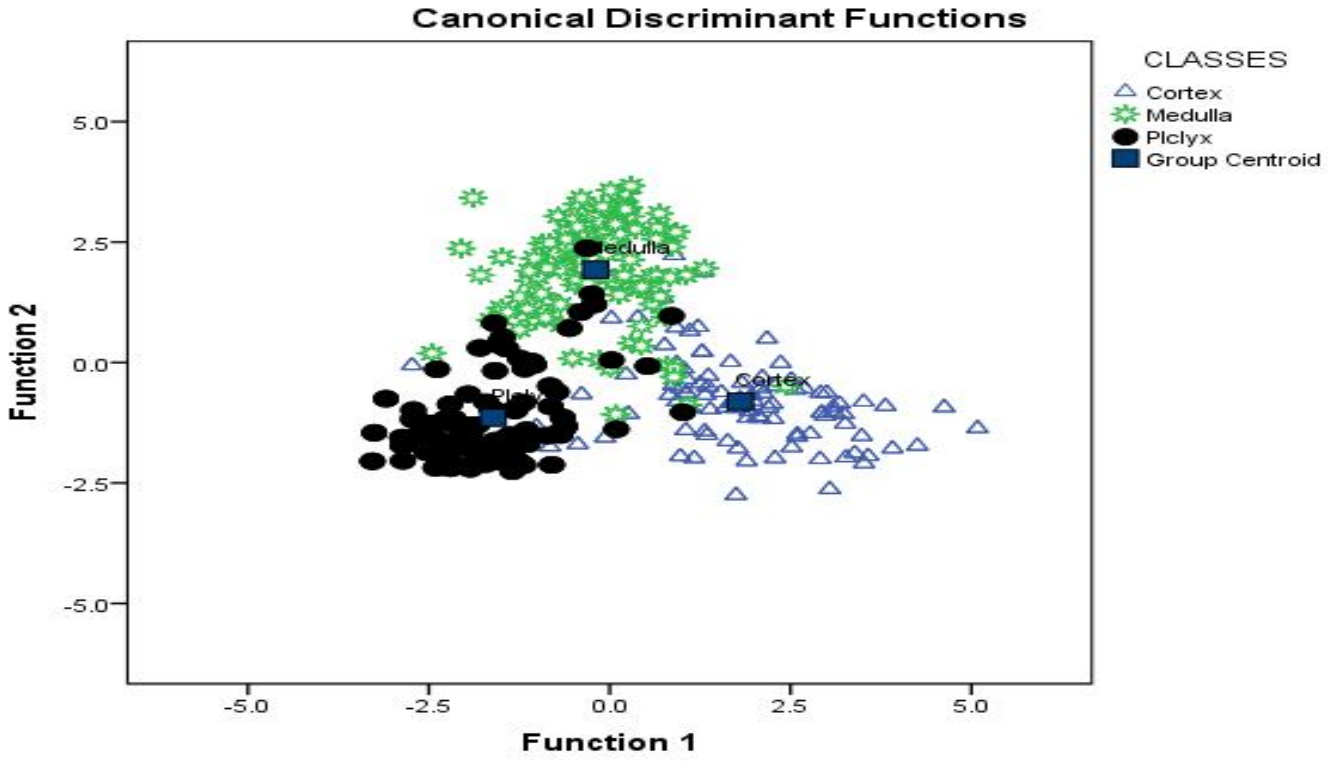

Fig (4.11) a scatter plot portrayed the class centers with the member of the class around it versus the discriminate function.

CLASSES		Predicted Group Membership			Total
		Cortex	Medulla	Pelvis	
Count	Cortex	170	14	14	198
	Medulla	10	181	10	201
	pelvis	4	16	178	198
%	Cortex	85.9	7.1	7.1	100.0
	Medulla	5.0	90.0	5.0	100.0
	Pelvis	2.0	8.1	89.9	100.0

Table (4-3) a confusion matrix shows the result of classification using linear discriminant analysis method.

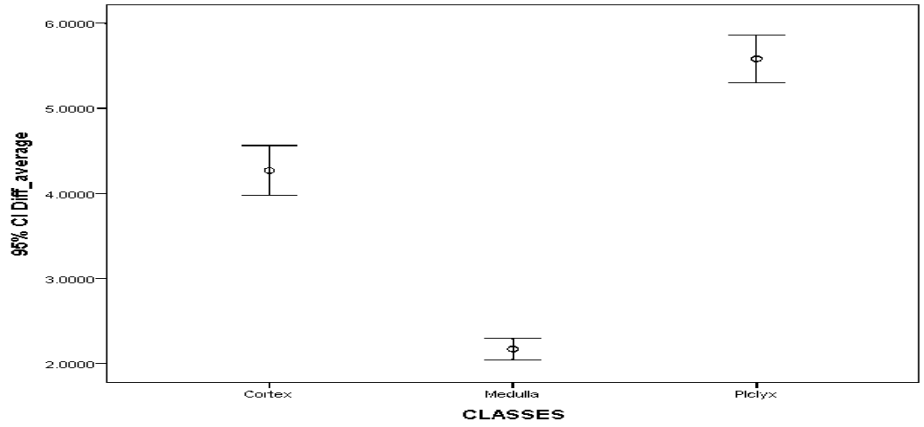

(a)

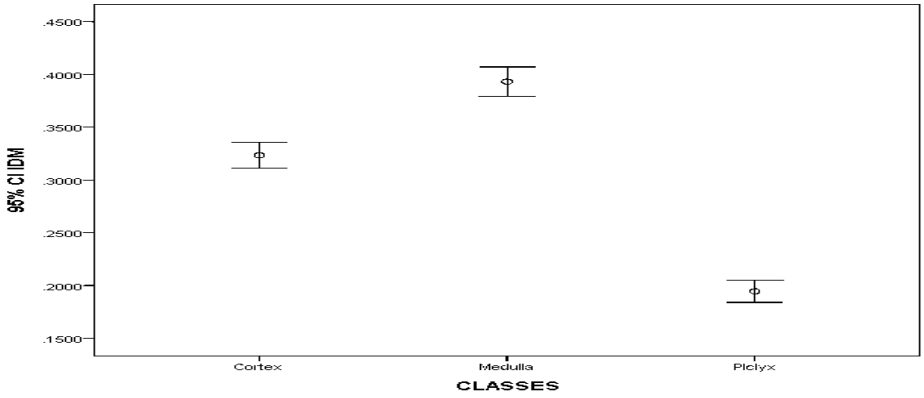

(b)

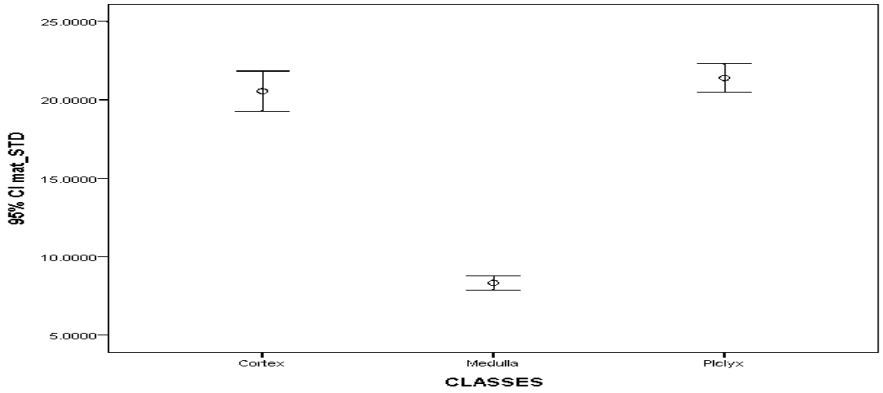

(C)

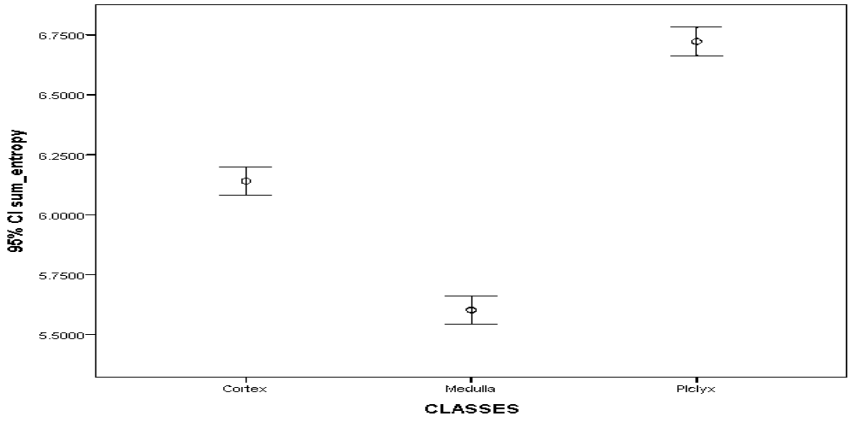

(D)

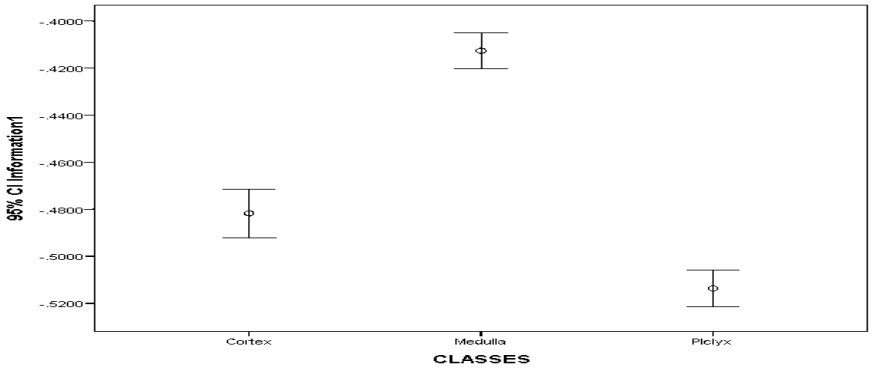

(E)

Fig(4.12) error bar plot of the feature victor for the three classes (cortex, medulla and pelvis) for the five discriminate selected features; (A) difference average, (B) inverse different moment, (C) SGLD matrix standard deviation, (D) sum entropy and Information correlation measure 1.

Chapter Five
(Discussion & Conclusion)

5-1 Discussion:

5-1-1 kidney measurement:

Renal length and volume measurements are clinically relevant, serving as surrogates for renal functional reserve, and are used frequently as the basis for making clinical decision. Serial measurements also can provide information regarding disease progression or stability.

The aims of this study were to establish reference values and define the normal kidney length and volume of Sudanese adults using MRI as well as to determine the relationship between kidney character and Sudanese body indices.

Correlations between measurements of the kidney and body indices were calculated. The data are expressed as means ± SD. Kidney length and volume were analyzed separately for males and females as well as the total sample. The data collection was assembled using EXCEL software programme and statistical analyses were performed using the impendent sample t-test, simple correlations (SPSS software version 16. USA).statistical significance was assumed at $P \leq 0.05$.

Table [4.1] showed the demographic data of the whole sample including weight, age, body surface area (BSA).body mass index, height, total body water (TBW),serum Creatinin, Creatinin clearance , Glomerular filtration rate (GFR).the kidneys volume and length for the total sample were measured and also for male and females subjects as presented in tables (Bartum.R. et al-1974;McRae .F. et al-1974).

The kidneys volume were found to be in the ranges from (80.32-122.91) with mean = 101.6±12.98 and (82.56-126.54) with mean 104.0 ±12.99 for the right and left

kidney .the males' kidney volume exceeded the volume of females by (1.79 and 4.09) for right and left kidneys . Right and Left kidney volume have significant relation p=0.000 with gender. The measurements of kidneys volume differs from other population (Kang.K. et al 2000; Shin .H. et al 2011.

The cause of this difference is may be due to the method of measurements or other factors. In the literature it was noted that the sonographic measurements of renal volume are very inaccurate (Bakkar .J. et al 1999; Emammian.SA. et al 1995; Sargent.MA. et al 1997) the volume of kidneys can be accurately measured by CT scanning with errors of 3% or less (Heymsfield SB. et al 1979) however, studies to data have measured total kidney volume, which includes tissue that does not contribute to renal function. The justification that the male has greater kidney volume then female is that the occurrence of larger glomeruli in men is solely dependent on their greater body surface area than females (Neugarten.J. et al 2002). the effect of gender on renal character may be due to a direct action of sex steroids on kidney growth or is secondary to differences in body composition, or other factors . measuring body mass index has shown enhanced correlation with adult renal volume (p=0.007,0.009) for right and left renal volume than body surface area (p=0.207,0.209) This agreed with the study done in children and adult RT and LT kidney volume correlates more strongly with the body size the with age (0.544,0.575) this also consigned to the study findings done in children (Johnson .S. et al 2011) this , together with the fact that BSA are closely linked in adults, suggests into adulthood(Mahajan .S. et al 2005).

Renal length determination is common everyday radiology practice. However, a normal range of kidney sizes may not apply to people of all body habitués. This study investigates this relationship in order to determine normal ranges in relation to body habitués.

Kidney lengths were measured the patients had normal Serum Creatinin levels, Creatinin clearance with no history of renal disease, no renal masses, and normal-appearing kidneys on MR T_1 Weighted images. The patients information were recorded, the mean renal length was 10.18±0.46, 10.67± 0.47 for RT and LT kidneys respectively. Males have mean length 10.23±0.49 and 10.7±0.46 and females have mean kidneys length=10.14±0.44,10.6±0.5 for RT and LT kidney length correspondingly. Statistical analysis demonstrated a relationship between kidney length and body weight and height, BMI , BSA, CrCl, GFR. The significant relation was found between the kidney length and body height. Additionally, kidneys lengths were generally larger in the males than females that means Normal renal length varies according to patient's body habitués(Neugarten.J. et al 2002)..

Both kidney volume and kidney length were significantly correlated to body indexes (BMI, Height, TBW) at value = 0.013, 0.021 for TBW with RT and LT volume and 0.007, 0.009 the BMI with RT and LT volume, 0.000, 0.000 the height with right and left volume and then 0.007, 0.000 the height with right and left kidney length fig (4.5) (4.6) an equations were established to predict the kidneys volume length and volume when the Sudanese BMI, TBW Height are well known. We also evaluated the predictability of kidney volume and kidney length to renal function, by using the CG equation which is regarded as accurate and less biased equation to estimate GFR in healthy adults (Mahajan .S. et al 2005;Al-Khader AA et al 2008).

Our study showed that there is significant relation between the CrCl, GFR, SrCr level with weight, BSA, BMI, age, TBW, gender. The result **revealed that the ki**dney volume predicted the renal function significantly SrCr 0.056,0.007, CrCl 0.054, 0.043, GFR 0.051, 0.59 for right and left kidneys volumes whereas the kidney length did not.

The study concluded that renal length and volume for Sudanese subject differed from other populations and between males and females and the volume can predict the renal function significantly, body habitués has an impact in kidney length .equations to predict Sudanese renal length and width were built up and reference values were established.

5-1-2 texture analysis:

The textual feature that extracted using 20×20 pixels window gives the best classification accuracy (fig 4.10) because this window is big enough to quantize the textural feature inside that window; where the texture is of a global nature than a very restricted area.

The linear discriminate analysis stepwise method selected five textural features out of 15 as the most discriminate one where they are well correlated with the class label as well as they show no co-linearity and hence they potentially possess a power of distinguishing the separate class as shown in fig (4.11) where the classes were well separated with an overall accuracy of 88.6% table (4.3).

The medulla showed highest classification accuracy because texturally it is very different than the cortex or pelvis. It has a hypotense structure while the result shares a hypertense structure.

The error in classification mostly arises when the extracting window overlapped two textural areas (two classes) near the borders. If the size of the window decreases the power of texture goes down while when it is big enough it might

include in the margin other texture; but still the 20×20 pixel window gives the best classification accuracy.

The textural feature difference average clearly differentiate the texture of the medulla from the pelvis and cortex with a minimum standard deviation Fig (4-12)(A) as well as the SGLD matrix standard deviation(C), (D) sum entropy. The cortex and pelvis were differentiated by the feature some entropy (D) as well from the medulla. The five feature together reduces the between class variance as well as they increases the between class variance; to minimizes the classification accuracy error.

5-2 Conclusion:

Correlations between measurements of the kidney and body indices were calculated.

The kidneys volume were found to be in the ranges from (80.32-122.91) with mean = 101.6±12.98 and (82.56-126.54) with mean 104.0 ±12.99 for the right and left kidney .the males' kidney volume exceeded the volume of females by (1.79 and 4.09) for right and left kidneys .

The mean renal length was 10.18±0.46, 10.67± 0.47 for RT and LT kidneys respectively. Males have mean length 10.23±0.49 and 10.7±0.46 and females have mean kidneys length=10.14±0.44,10.6±0.5 for RT and LT kidney length .

This variation can be expressed as a function of body height, which can be represented by an equation and used as an easy reference in clinical practice.

- *Left kidney length = 0.038height+3.940 R^2= 0.128.* Eq (27)
- *Right kidney length = 0.028height+5.202 R^2= 0.073.* Eq (28)
- *Right kidney volume = 1.702height -198.9 R^2=0.347.* Eq (29)
- *Left kidney volume = 1.667xheight+190.2 R^2=0.332.* Eq (30)

Texture analysis can provide useful information about the microstructure of the organ of interest, this means a system using texture analysis to classify the kidney tissues into cortex, medulla and pelviocalyceal system can speed the process of diagnosis. Therefore main objective of this study was to use texture analysis techniques in order to identify the pathologically kidney from the normal one.

Textural analysis used to classify the normal kidney into three classes as cortex Medulla and pelvis showed a classification accuracy of 88.6%; where the error of classification mainly attributed to the size of the window, which superimposed on more than one textures. To classify unseen images into the three classes using linear discriminate analysis we can apply the following equation:

- Cortex:

[(energy *449723.50)+(inertia*-0.237)+(IDM*-2.84.78)+(correlation-367.73)+(sum average*2.45)+(sum entropy*53.71)+(sum variance*.153)+(infro1*4431.47)+(infro 2*41308.43)+(mat-STD*-22.42)+(-19891.8)]. Eq (31)

- parenchyma :

[(energy *45208.31)+(inertia*-0.188)+(IDM*-321.50)+(correlation*-439.76)+(sum average*2.38)+(sum entropy*55.98)+(sum variance*.158)+(infro 1*4421.57)+(infro 2*41203.15)+(mat-STD*-24.11)+(-19838.08)]. Eq (32)

- Pelviocalyceal system :

[(energy *45966.09)+(inertia*-.220)+(IDM*-354.50)+(correlation*414.80)+(sum average*2.36)+(sum entropy*61.84)+(sum variance*-.155)+(infro 1*4398.72)+(infro 2*41178.44)+(mat-STD*-23.37)+(-19836.16)]. Eq (33)

The textural feature difference average, inverse difference moment IDM, SGLD matrix standard deviation, sum entropy, Information correlation measure 1. The five feature together reduces the between class variance as well as they increases the between class variance; to minimizes the classification accuracy error.

5-3 Recommendations:

- ✓ Use the sense coil for T_1 image to improve image quality but consider for time of exam.
- ✓ Increase number of slice in FOV and use less than 3.00mm slice thickness and decrease gap between slice to more accurate measurement.
- ✓ Obtain classification using neural Network technique.
- ✓ Compare the classification result with result obtained using neural Network technique.
- ✓ Use texture descriptors derived from volumetric data to aid the Classification in MRI.

5-4 limitation:

- ✓ Difficult to provide MR examination of the urinary system and abdomen in general.
- ✓ There is no fixed protocol for the UT imaging in MRI.
- ✓ High cash cost which affects the possibility of conducting the examination.